DISSERTATION

Function and regulation of mast cells in the inner ear and applications to mast cell-driven diseases

Funktion und Regulation von Mastzellen im Innenohr und Anwendungen bei Mastzellen-bedingten Krankheiten

zur Erlangung des akademischen Grades
Doctor medicinae (Dr. med.)

vorgelegt der Medizinischen Fakultät
Charité – Universitätsmedizin Berlin

von
Bin Zeng

Erstbetreuung: Prof. Dr. med. Frank Siebenhaar

Datum der Promotion: 20.June 2025

Table of Contents

List of Tables

List of Figures

List of Abbreviations

BMMC: Bone marrow-derived mast cell

BSA: Bovine serum albumin

CCL: Chemokine (C-C motif) ligand

c-Kit: Tyrosine-protein kinase Kit (CD117)

CO2: Carbon dioxide

CP48/80: Compound 48/80

CTMC**:** Connective tissue-type mast cell

CXCL: Chemokine (C-X-C motif) ligand

dH2O: Distilled water

DMEM/F12: Dulbecco's Modified Eagle Medium/Nutrient Mixture F12

DMSO: Dimethyl sulfoxide

DNA: Deoxyribonucleic acid

DNP: Dinitrophenyl-albumin

EDTA: Ethylenediamine tetraacetic acid

ELISA: Enzyme-linked immunosorbent assay

MEM: Minimum Essential Medium

FCS: Fetal calf serum

FcεRI: Fc-epsilon receptor

FGF: Fibroblast growth factor

GM-CSF: Granulocyte-macrophage colony-stimulating factor

IFN-α/β: Interferon-α/β

IFN-γ: Interferon-γ

IgE: Immunoglobulin E

IHC: Inner hair cell

IL: Interleukin

LW: Lateral wall

MC: Mast cell

Mcpt: Mast cell protease

MC_T: Tryptase-expressing mucosal mast cell

MC_{TC}: Tryptase- and chymase-expressing connective tissue mast cell

Min: Minutes

MMC: Mucosal mast cells

NGF: Nerve growth factor

OC: Organ of Corti

OHC: Outer hair cell

P/S: Penicillin/Streptomycin

PBS**:** Phosphate-buffered saline

ROS: Reactive oxygen species

SCF: Stem cell factor

SD: Standard deviation

SGN: Spiral Ganglion Neuron

SL: Spiral Ligament

SV: Stria vascularis

TGF-β: Transforming growth factor-beta

TNF: Tumor necrosis factor

VEGF: Vascular endothelial growth factor

Abstract

Mast cells (MCs) are crucial immune cells and have been widely recognized as key effector cells in the induction of allergic symptoms. In this study, cochlear tissue from p3-5 C57BL/6 mice was used as an *in vitro* model to investigate the morphological effects of MC degranulation on the mouse cochlea and the activation capacity of resident cochlear MCs. The results revealed significant and dose-dependent impairments in cochlear morphology and hair cell numbers following 24-hour co-culture with degranulated bone marrow-derived mast cell (BMMC) supernatant. Moreover, chymase and tryptase were detected in the cochlear tissue supernatant after 1 hour of treatment with Compound 48/80 at concentrations of 20 µM, 50 µM, and 100 µM. Notably, a range of proinflammatory cytokines (including GM-CSF, IFNy, IL-6, IL-18, and TNF) was observed in the cochlear tissue supernatant after 1-hour treatment. Additionally, time-course experiments with 15 µM cisplatin revealed a time-dependent release of histamine and tryptase. The present study highlights the complexity of MC biology and its importance in the inner ear immune response and reveals a potential mechanistic link between inner ear dysfunction and MC-driven disease. It also demonstrates that resident cochlear MCs possess the ability to degranulate and suggests that they may play a role in cisplatin-induced ototoxicity and that the pathological effects induced by MCs may even precede cisplatin-induced reactive oxygen species (ROS) accumulation. Future studies are needed to reveal the exact mediators and signalling cascades involved in MC-mediated cochlear injury.

Zusammenfassung

Mastzellen (MCs) sind wichtige Immunzellen und gelten seit langem als Schlüsselzellen bei der Auslösung von allergischen Symptomen. In dieser Studie wurde Cochlea-Gewebe von p3-5 C57BL/6-Mäusen als *In vitro*-Modell verwendet, um die morphologischen Auswirkungen der MC-Degranulation auf die Cochlea der Maus und die Aktivierungskapazität der in der Cochlea ansässigen MCs zu untersuchen. Die Ergebnisse zeigten signifikante und dosisabhängige Beeinträchtigungen der Morphologie der Cochlea und der Anzahl der Haarzellen nach 24-stündiger Co-Kultur mit Überstand von degranulierten *in vitro* differenzierten Mastzellen aus dem Knochenmark (BMMC). Außerdem wurden Chymase und Tryptase im Überstand des Cochlea-Gewebes nach einer einstündigen Behandlung mit Compound 48/80 in Konzentrationen von 20 µM, 50 µM und 100 µM , sowie eine Reihe von pro-inflammatorischen Zytokinen (einschließlich GM-CSF, IFNy, IL-6, IL-18 und TNF) nachgewiesen. Darüber hinaus zeigten Zeitverlaufsexperimente mit 15 µM Cisplatin eine zeitabhängige Freisetzung von Histamin und Tryptase. Die vorliegende Studie verdeutlicht die Komplexität der MC-Biologie und ihre Bedeutung für die Immunreaktion im Innenohr und zeigt eine mögliche mechanistische Verbindung zwischen Funktionsstörungen des Innenohrs und MC-bedingten Krankheiten auf. Sie zeigt auch, dass die in der Cochlea ansässigen MCs die Fähigkeit zur Degranulation besitzen, und deutet darauf hin, dass die in der Cochlea ansässigen MCs eine Rolle bei der Cisplatin-induzierten Ototoxizität spielen und dass die durch MCs induzierten pathologischen Effekte sogar der Cisplatin-induzierten Akkumulation reaktiver Sauerstoffspezies (ROS) vorausgehen können. Zukünftige Studien sind erforderlich, um die genauen Mediatoren und Signalkaskaden aufzudecken, die an der MC-vermittelten Schädigung der Cochlea beteiligt sind.

1. Introduction

1.1 Mast cells

Mast cells (MCs) are a type of immune cell present in all vertebrates, having evolved long before the development of the adaptive immune system hundreds of millions of years ago (Mulero, Sepulcre et al. 2007). The history of MC research began in 1878 when Paul Ehrlich, a physician and researcher, first described and named the aniline-reactive granulocytes he found in connective tissue as mast cells (Mastzellen) in his doctoral dissertation (Ehrlich 1877). MCs have been the object of study and have drawn the attention of countless researchers since then, leading to a substantial increase in our knowledge of their intriguing biology and function.

1.1.1 Characterization of mast cells

MCs are characterized by their distinctive granules, which contain various bioactive molecules such as preformed mediators (histamine, chymase, and tryptase), and a wide range of cytokines and other chemokines which can be synthesized after activation of the cell by IgE and antigens, or other stimuli.

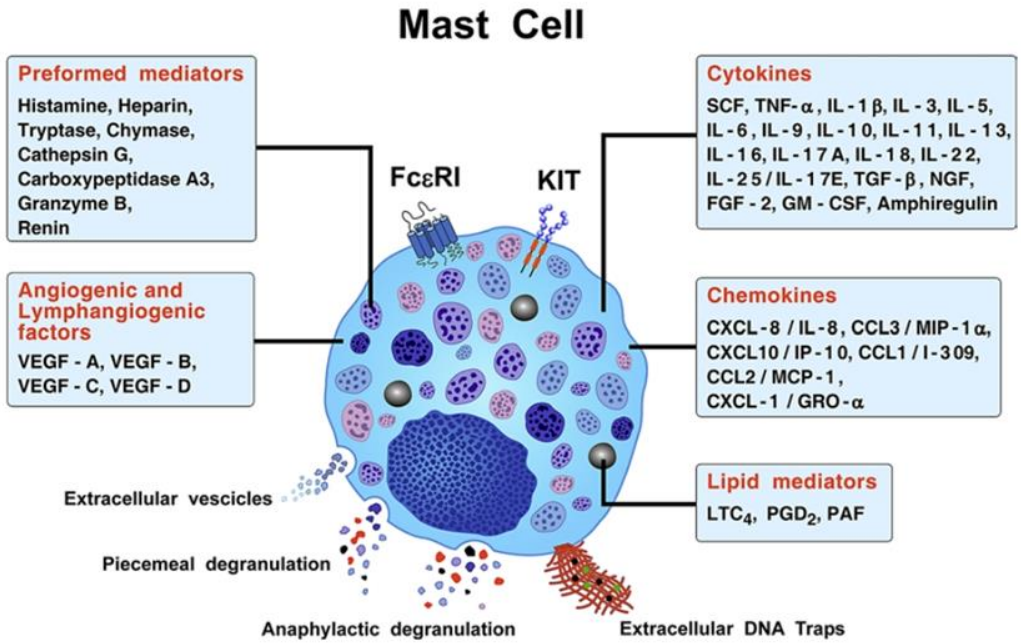

Figure 1. Proinflammatory and immunomodulatory mediators of human MCs. (Varricchi, Rossi et al. 2019)

On the surface of MCs, there is a range of receptors expressed, such as high-affinity IgE receptor (FcεRI), stem cell factor receptor (c-kit), pathogen-recognizing Toll-like receptors (TLR), and MAS-related G-protein-coupled receptor X2 (MRGPRX2). Activation of these receptors can initiate MC activation, resulting in the secretion of proinflammatory and immunomodulatory mediators.

1.1.2 Development, distribution, and heterogeneity of mast cells

MCs originate from pluripotent hematopoietic stem cells (Chen, Grimbaldeston et al. 2005, Kitamura, Oboki et al. 2007), and they stay as undifferentiated progenitor cells while circulating through the bloodstream until entering peripheral tissue, where they ultimately undergo maturation (Kitamura, Sonoda et al. 1985, Kitamura, Kasugai et al. 1993). Mature MCs are distributed across various connective and mucosal tissues, as well as within all vascularized organs. Their highest concentrations occur at interfaces between internal and external environments, facilitating responsiveness to antigens and foreign organisms, thereby serving as the sentinels (Metcalfe, Baram et al. 1997, Galli, Kalesnikoff et al. 2005). This deliberate distribution ensures a rapid response through the release of mediators and recruitment of immune cells to the targeted sites of action (Galli, Maurer et al. 1999, Abraham and St John 2010).

The maturation, phenotype, and functionality of MCs are considered to be directly influenced by the surrounding microenvironment (Galli, Borregaard et al. 2011). This microenvironment, which includes stem cell factor (SCF) and other cytokines (e.g. IL-3, IL-9), plays a crucial role in regulating the growth, differentiation, and maturation process of MCs (Metcalfe, Baram et al. 1997, Jamur and Oliver 2011). Mice with spontaneous double mutations in the kit gene, which encodes the SCF receptor (c-Kit), exhibit a near-complete absence of MCs. WBB6F1-Kit^{W}/Kit^{W-v} (Kit^{W}/Kit^{W-v}) mice, characterized by deficient c-Kit expression, demonstrate a marked absence of MC development, mild anemia, complete melanocyte deficiency, and sterility (Galli and Kitamura 1987). Another MC-deficient mouse strain, C57BL/6-Kit^{W-sh}/Kit^{W-sh} (Kit^{W-sh}), also lacking MCs and melanocytes, presents fewer abnormalities than the Kit^{W}/Kit^{W-v} mice (Grimbaldeston, Chen et al. 2005, Wolters, Mallen-St Clair et al. 2005). These MC-deficient mice models have become invaluable tools for *in vivo* studies of MC function.

Based on the anatomical distributions, murine MCs are categorized into two primary subsets: connective-tissue MCs (CTMC), predominantly situated proximate to vessels and nerve endings in most connective tissues, and mucosal MCs (MMC), mainly found in the epithelium of the mucosa of the gastrointestinal tract and respiratory tract (Enerbäck 1966). In humans, MCs can also be defined as tryptase-expressing mucosal MCs (MC_T) and tryptase- and chymase-expressing connective tissue MCs (MC_{TC}) according to the different levels of two key granule-associated proteases (Craig and Schwartz 1989). Table 1 below shows the properties of mouse and human MCs (St. John, Rathore et al. 2023).

Table 1. Characteristics of mouse and human MCs (St. John, Rathore et al. 2023)

Property	**Mouse MCs**	**Human MCs**
Main subsets	CTMC	MC_{TC}
	MMC	MC_T
Major proteoglycan in granules	Heparin for CTMC; chondroitin sulfate for MMC	Heparin for CTMC; chondroitin sulfate for MMC
Expression of IgE receptor (FcεRI)	Low or no expression on fetal MC; increased expression with gestational age	Low or no expression on fetal MC; increased expression with gestational age. Higher levels of expression on fetal skin MCs compared with fetal lung MCs.
Cytokines, chemokines, and growth factors reported as produced	IL-1β, IL-2, IL-3, IL-4, IL-5, IL-6, IL-9, IL-10, IL-12, IL-13, IL-15, IL-17, IL-33, TNF, FGF, GM-CSF, IFN-γ, IFN-α/β, TGF-β, VEGF, CCL1, CCL2, CCL3, CCL4, CCL5, CCL6, CCL7, CCL8, CCL9, CCL17, CCL20, CCL22, CCL25, CCL27, CXCL1, CXCL2, CXCL8, CXCL10, CXCL12, CX3CL1	IL-1β, IL-2, IL-3, IL-4, IL-5, IL-6, IL-10, IL-11, IL-12, IL-13, IL-15, IL-16, IL-17a, IL-18, TNF, FGF, GM-CSF, IFN-γ, IFN-α/β, TGF-β, VEGF, CCL1, CCL2, CCL3, CCL4, CCL5, CCL6, CCL7, CCL8, CCL11, CCL16, CCL17, CCL18, CCL20, CCL22, CCL23, CXCL1, CXCL2, CXCL3, CXCL6, CXCL8, CXCL9, CXCL10

Major proteases	Mcpt1–7 and carboxypeptidases; Mcpt4 is a chymase, Mcpt6 and Mcpt7 are tryptases. MCTC express more Mcpt4, Mcpt5, Mcpt6 and carboxypeptidase A3, whereas MMC express more Mcpt1 and Mcpt2, although heterogeneity exists both within and between tissues.	Tryptase, chymase, and carboxypeptidase
Biogenic amines produced	Serotonin, histamine, and dopamine	Serotonin and histamine; dopamine unreported
Neuropeptides produced	Substance P, vasoactive intestinal polypeptide, and NGF	Substance P, vasoactive intestinal polypeptide, and NGF

1.1.3 Activation and function of mast cells

The activation of MCs can be described as being FcεRI-dependent and FcεRI-independent (Metcalfe, Baram et al. 1997). FcεRI, a high-affinity IgE receptor, is considered to be one of the most important receptors expressed on the MC surface. It consists of a heterotetrametric structure, comprising an IgE-binding α-subunit, a β-subunit with four transmembrane spans, and two γ-subunits connected by disulfide bonds (Kinet 1999, Kawakami and Galli 2002). Initiation of the activation process occurs through the interaction between a multivalent antigen (allergen) and its corresponding specific IgE antibody, which is tethered to the cell membrane via the FcεRI receptor, leading to the rapid release of pre-formed proinflammatory and immunomodulatory mediators from the granules (Metcalfe, Baram et al. 1997, Nadler, Matthews et al. 2000, Kawakami and Galli 2002). This process is considered as the central event in acute allergic reactions and the development of symptoms (Galli and Tsai 2012). In addition to activation by IgE and antigen, a variety of alternative substances can evoke the release of MC mediators through FcεRI-independent pathways. These substances include polybasic molecules (e.g., Compound48/80 (CP48/80), mastoparon, and polymyxin B), peptides (e.g. Substance P), complement fragments (e.g. C5a), cytokines, and other stimuli (Metcalfe, Baram et al. 1997). Additionally, cisplatin, a frequently used chemotherapy medication for treating

diverse cancers, has demonstrated the ability to trigger MC activation (Brzezińska-Błaszczyk, Mińcikiewicz et al. 1996).
In this study, the mouse IgE-anti-dinitrophenyl (DNP) and DNP system, a well-established model for investigating IgE-mediated responses, was utilized. Mouse IgE-anti-DNP is a monoclonal antibody that specifically binds to DNP haptens. These IgE antibodies are produced by immunizing mice with DNP-conjugated proteins, leading to the generation of hybridomas that secrete high-affinity anti-DNP IgE. The binding of DNP and IgE-anti-DNP triggers the activation and degranulation of MCs (Eshhar, Ofarim et al. 1980, Bohn and König 1982, Bohn and König 1982).

Upon activation, a wide range of active mediators are released from MCs, triggering a series of biological effects (Metcalfe, Baram et al. 1997, Boyce 2003, Marone, Triggiani et al. 2005, Metz and Maurer 2007). MC-dependent mediators can be classified into three categories: preformed secretory granule-associated mediators, lipid-derived mediators, and cytokines (Metcalfe, Baram et al. 1997). Histamine is one of the most typical MC-preformed secretory granule-associated mediators, the release of which leads to vasodilation, smooth muscle contraction, bronchoconstriction, as well as heightened capillary permeability (Lundequist and Pejler 2011). The proteoglycans and proteases (e.g., chymase and tryptase) are also preformed mediators stored in the cytoplasmic granules. MC granule protease phenotypes are classified by the fact that MCs of different species and developmental stages exhibit different combinations of granule proteases (Table 1). In addition, MC activation can synthesize and secrete lipid-derived substances (e.g., cyclooxygenase and lipoxygenase metabolites of arachidonic acid) and a variety of cytokines, such as granulocyte-macrophage colony-stimulating factor (GM-CSF), tumor necrosis factor (TNF) and IL-2, IL-3, IL-4, IL-5 and IL-6, as well as Interferon gamma (IFN-γ), which further promote the inflammatory response and cell-cell interactions (Metcalfe, Baram et al. 1997).

Due to the release of these biologically active mediators, MC activation is not only involved in the regulation of immune responses but also plays an important role in the pathogenesis of inflammation and allergy (González-de-Olano and Álvarez-Twose 2018), urticaria (Church, Kolkhir et al. 2018), as well as other disorders, such as inflammatory bowel disease (Dvorak, Monahan et al. 1980, Roberts-Thomson, Fon et al. 2011), fibrinolysis (Strattan, Palaniyandi et al. 2019), and lung diseases (Virk, Arthur et al. 2016).

1.2 Inner ear

1.2.1 Inner ear anatomy

In mammals, the inner ear comprises two distinct functional components. Firstly, the vestibular system, along with the vestibule and semicircular canals, is the sensory system responsible for maintaining balance. Secondly, the cochlea, converting sound pressure impulses originating in the outer ear and transformed into mechanical energy in the middle ear into electrical signals transmitted to the central auditory system through the auditory nerve, is responsible for the sense of hearing (Fettiplace and Kim 2014, Ekdale 2016, Fettiplace 2017).

1.2.2 The cochlea

Auditory signal transduction occurs within the cochlea, a spiral-shaped structure located in the ventral portion of the inner ear. The cochlea comprises three ducts: the scala vestibuli, scala media (cochlear duct), and scala tympani (Ekdale 2016, Driver and Kelley 2020). Both the scala vestibuli and scala tympani are filled with perilymph. They are connected at the apex of the cochlea, which is known as the helicotrema. In contrast, the cochlear duct and membranous vestibular apparatus contain endolymph (Braun, Böhnke et al. 2012, Ekdale 2016). The composition of perilymph is characterized by high sodium and low potassium content, resembling extracellular fluid (Sterkers, Ferrary et al. 1988). In contrast, the endolymph has significantly higher potassium and lower sodium content, with a composition comparable to intracellular fluid (Bosher and Warren 1968, Sterkers, Ferrary et al. 1988, Payan, Kossmann et al. 1997). The pressure and volume of endolymph influence both vestibular and auditory functions. For instance, an increased volume of endolymph, also known as endolymphatic hydrops, is highly associated with Meniere's disease, characterized by hearing loss and vertigo (Havia, Kentala et al. 2002).

The scala media is apically separated from the adjacent scala vestibuli by Reissner's membrane (RM) (Driver and Kelley 2020), and basally by the osseous lamina and the basilar membrane, which separate the cochlear duct from the scala tympani. The organ of Corti (OC) is located on the surface of the basilar membrane in the cochlear duct (Ekdale 2016). The stria vascularis (SV) forms the lateral wall (LW) of the cochlear duct

with the spiral ligament (SL), and is a highly vascularized tissue responsible for the production of endolymph (Fay 2012).

1.2.3 The organ of Corti and hair cells

The OC is composed of two types of hair cells (HC), namely inner hair cells (IHCs) and outer hair cells (OHCs), which are responsible for auditory sensation transduction. Additionally, several non-sensory supporting cell types, including inner phalangeal cells, pillar cells, Hensen's cells, and Deiters' cells, among others, contribute to its structure. The arrangement of HC and supporting cells forms a precisely ordered cellular mosaic, extending along the basal-to-apical (tonotopic) axis of the cochlea (Driver and Kelley 2020).

As the sensory receptors of the auditory system, each HC is comprised of mechanically sensitive bundles of stereocilia situated on its luminal surface. These bundles typically contain 50-200 individual stereocilia organized in rows, forming a V-shape, with their length increasing in a stair-like pattern (Driver and Kelley 2020). OHC and IHC have different numbers, positions, and functions in the cochlea. More than 3/4 of the sensory cells are OHCs (Fay 2012), and they are positioned on the lateral side of the tunnel of Corti, whereas IHCs, as their name indicates, are situated on the inner side. The potential of OHCs correlates with basilar membrane displacement, whereas the potential of IHCs shows a positive correlation with the basilar membrane vibration rate (Dallos, Billone et al. 1972, Fettiplace and Hackney 2006).

1.2.4 Auditory physiology and dysfunction of the inner ear

Auditory transduction, the process of converting sound waves into electrical signals that the brain recognizes and processes, begins with the sound waves that hit the eardrum through the external ear canal and cause vibration (Lim and Brichta 2016). These vibrations are transmitted to the oval window of the cochlea through the three small bones of the middle ear (hammer, incus (anvil), and stapes), also known as the auditory ossicles (Lim and Brichta 2016). The perilymph oscillates within the vestibule, producing pressure waves propagating to the endolymph (Lim and Brichta 2016). The resultant shear force bends the three-dimensional cilia of the HCs (Lim and Brichta 2016). The mechanical displacement of the hair bundles induces depolarization, triggering the contraction of the

OHCs through an electrokinetic process (Yoshioka and Sakakibara 2013, Lim and Brichta 2016). At the same time, the mechanically gated potassium channels on the apical stereocilia of the HCs open in response to vibration, resulting in the release of the neurotransmitter glutamate, which stimulates the nerve fibers at the base of the HCs (Yoshioka and Sakakibara 2013, Lim and Brichta 2016, Altoè, Pulkki et al. 2018). These nerve fibers transmit auditory information via the cochlear nerve to the auditory brainstem, where it is ultimately processed and interpreted in the auditory region of the temporal lobes. Different auditory frequencies stimulate the HCs located in corresponding, specific regions along the cochlea, with the high oscillatory frequencies being perceived at the base of the cochlea and the low frequencies at the tip of the cochlea (Mann and Kelley 2011).

Auditory dysfunctions manifest primarily as hearing loss. Besides age-related hearing loss, the most common etiology is damage to the HCs caused by exposure to noise, and the consequent loss of the ability to perceive different frequencies (Rabinowitz 2000, Goines and Hagler 2007). Noise exposures that induce only temporary shifts in hearing thresholds have reversible effects on the function of HCs. These functional alterations are correlated with the recovery of hearing thresholds and the repair of structures such as stereocilia. In contrast, exposure to higher levels and/or prolonged periods of noise can inflict permanent damage on HCs, potentially leading to the death of HCs and resulting in permanent threshold shifts (Shi, Chang et al. 2016). Besides noise, drugs such as aminoglycoside antibiotics (e.g. gentamicin), chemotherapeutic agents (e.g. cisplatin), loop diuretics (e.g. furosemide), and antimalarials (e.g. chloroquine) may also have an inner-ear-damaging effect, which can result in hearing loss and tinnitus in patients (Lanvers-Kaminsky, Zehnhoff-Dinnesen et al. 2017). In addition, epidemiologic evidence supports an association between allergic diseases and specific inner ear disorders, suggesting that a high prevalence of allergic reactions may cause or worsen hearing loss and tinnitus (Zeng, Domarecka et al. 2024).

1.3 Cisplatin ototoxicity and its effect on mast cells

Cisplatin is a widely used chemotherapy medication for the treatment of various malignant tumors (Kelland 2007). One mechanism by which cisplatin directly induces apoptosis is through the formation of covalent compounds on the nitrogen atoms of guanine and adenine. This process leads to interstrand cross-links in the DNA strand, which

subsequently impairs replication and transcription (Heiger-Bernays, Essigmann et al. 1990, Jordan and Carmo-Fonseca 2000, Wang and Lippard 2005). Ototoxicity is one of the major side effects of cisplatin and manifests as bilateral, dose-dependent progressive, irreversible sensorineural deafness, starting in the high frequencies and progressing to the low frequencies (Rybak 2007, Brock, Knight et al. 2012). Auditory HCs are the main target cells for cisplatin-induced ototoxicity, especially OHCs (Brock, Knight et al. 2012). Cisplatin not only impairs HCs but also affects the vascular stria (SV) (Meech, Campbell et al. 1998) and spiral ganglion neurons (SGN) (Yu, Man et al. 2019). The precise mechanisms underlying cisplatin-induced ototoxicity, however, remain incompletely elucidated. Current research suggests that cisplatin can induce the generation of reactive oxygen species (ROS) within the cochlea, resulting in the depletion of antioxidant enzymes and ultimately exacerbating apoptosis (Rybak 2007, Gonçalves, Silveira et al. 2013). Moreover, cisplatin has been found to elevate the early immediate release and de novo synthesis of proinflammatory cytokines, such as TNF, IL-1beta, and IL-6 in cochlear *in vitro* cell line HEI-OC1 cells, indicating that proinflammatory cytokines may contribute to the pathophysiology of sensory hair cell (HC) damage induced by cisplatin (So, Kim et al. 2007).

A recent study has identified the presence of mast cells (MCs) in rodent cochlea (Szczepek, Dudnik et al. 2020, Karayay, Olze et al. 2023). Moreover, cisplatin induced the degranulation of MCs (Karayay, Olze et al. 2023), whereas the inhibition of MCs degranulation using cromolyn has been shown to protect against HC and SGN damage in cochleae exposed to cisplatin (Karayay, Olze et al. 2023). However, to our knowledge, there are no current studies examining the precise mechanism of action of resident cochlear MCs in cisplatin-induced ototoxicity.

1.4 Aims of the study

Building on the provided background, this study hypothesizes that under various conditions, mast cells (MCs) might contribute to the pathologies of the cochlea. To test this hypothesis, the following aims were identified:

1. To examine the impact of degranulation of murine bone marrow-derived MCs on cochlear morphology and hair cells.
2. To investigate the stimulatory capacity of mouse IgE-anti-DNP and DNP on resident MCs in the inner ear.
3. To assess the stimulatory capacity of Compound 48/80 on resident MCs in the inner ear.
4. To evaluate the stimulatory capacity of cisplatin on resident cochlear MCs.

2. Materials and Methods

2.1 Materials

2.1.1 Table 2. Laboratory equipment

Name	Manufacturer
Cell culture plate 4-well slide	Thermo Fisher Scientific, Waltham, USA
Centrifuge Megafuge 1.0 ST R	Heraeus, Hanau, DE
CO2-incubator HeraCell 150i	Thermo Fisher Scientific, Waltham, USA
Counting chamber Neubauer Improved	VWR International, Radnor, USA
Electronic pipette boy2	INTEGRA Biosciences, Hudson, USA
Fluorescence microscope EVOS FL Cell Imaging System Keyence BZ-X800	Thermo Fisher Scientific, Waltham, USA Keyence, Osaka, JPN
Freezer -20 °C Liebherr comfort	Liebherr, Biberach an der Ris, DE
Luminex MAGPIX system	Luminex, Texas, USA
Microwave R-208 Sharp	Sharp K.K., Osaka, JPN
Multi-channel pipette 5µl-50µl, 50µl-300µl	Eppendorf Research, Hamburg, DE
Plate reader VICTOR X	PerkinElmer, New Jersey, USA
Plate shaker Typ RO 10	Gerhardt GmbH & Co. KG, Königswinter, DE
Pipette PhysioCare variabel	Eppendorf Research, Hamburg, DE
Precision balance Sartorius 1-1000 mg	Sartorius AG, Göttingen, DE

SpectroMax M5 microplate reader (Molecular Devices)	Heidolph, Schwabach, DE
Stereomicroscope SteREO Discovery.V8	Carl Zeiss, Oberkochen, DE
Sterile bench LaminAir HBB 2448	Heraeus Holding GmbH, Hanau, DE
Sterile workbench Typ C424 H	CEAG Schirp, Burladingen, DE
Table centrifuge 5417R	Eppendorf Research, Hamburg, DE
Thermal shaker DTS-2	LTF Labortechnik GmbH & Co. KG, Wasserburg, DE
Refrigerator 4 °C	Liebherr Profiline, Liebherr, Biberach an der Ris, DE
Water bath WBT 222	Medingen, Dresden, Germany
Ultra-low temperature freezer -86 °C HERA freeze	Thermo Fisher Scientific, Waltham, USA
Vortexer IKA MS1	IKA®-Werke GmbH & Co. KG, Staufen, DE
xPONENT analysis software	Luminex, Texas, USA

2.1.2 Table 3. Reagents, chemicals, and buffers

Name	Manufacturer
Alexa Fluor™ 594 Phalloidin	Life technologies™, Carlsbad, USA
Alexa Fluor™ 488	Life technologies™, Carlsbad, USA
Ampuwa water	Fresenius Kabi, Bad Homburg, DE
Antibody diluent	Abcam (Cambridge, UK)
Cis-Diammineplatinum (II) dichloride, Cisplatin	Merck KGaA (Darmstadt, DE)
Compound 48/80	Sigma-Aldrich (St. Louis, USA)
D-(+)-Glucose solution	Sigma-Aldrich (St. Louis, USA)

DAPI	Sigma-Aldrich (St. Louis, USA)
Dimethylsulfoxide DMSO	SERVA Electrophoresis GmbH (Heidelberg, DE)
DMEM/F12	Gibco® by Life technologies™ (Carlsbad, USA)
Ethylenediaminetetraacetic acid EDTA	Merck, Darmstadt, Germany
Electrolyte infusion solution with glucose	Serumwerk Bernburg AG (Bernburg, DE)
Ethanol 96%	Merck KGaA (Darmstadt, DE)
Fetal bovine serum	Merck KGaA (Darmstadt, DE)
Formaldehyde solution 4% Formalin solution 10%	SAV LP GmbH (Flintsbach am Inn, DE) Sigma-Aldrich (St. Louis, USA)
H2O, steril	Braun, Melsungen, Germany
Insulin-like growth factor I	R&D Systems (Minneapolis, USA)
Natriumhydroxid NaOH	Merck, Darmstadt, Germany
PBS Tablets	Gibco® by Life technologies™ (Carlsbad, USA)
Penicillin G Sodium Salt	Merck KGaA (Darmstadt, DE)
Penicillin-streptomycin solution	Thermo Fisher Scientific (Waltham, USA)
ProLong™ Gold antifade reagent	Invitrogen by Thermo Fisher Scientific (Waltham, USA)
Recombinant Mouse IGF-1	R&D Systems (Minneapolis, USA)
RPMI 1640 Medium	Biochrom GmbH (Berlin, DE)
Sodium cromoglycate, cromoglicic acid	TargetMol (Boston, USA)
TritonTM X-100	Sigma-Aldrich (St. Louis, USA)
Wash Buffer	Cell Signaling (Cambridge, UK)

2.1.3 Table 4. Kits

Name	Manufacturer
ELISA kit for mouse Chymase (CMA1)	Cloud-Clone Corp (Katy, USA)
ELISA Kit for mouse Tryptase (TPS)	Cloud-Clone Corp (Katy, USA)

ELISA kit for Histamine (Colorimetric)	Novus Biologicals (Wiesbaden Nordenstadt, DE)
ProcartaPlex™ Mouse Th1/Th2 Cytokine Panel, 11plex	Thermo Fisher Scientific (Waltham, USA)

2.2 Methods

All studies were performed following the German Prevention of Cruelty to Animals Act and were approved by the Berlin Senate Office for Health. All experiments were carried out only by authorized persons and followed the 3R principle.

2.2.1 Mast cells isolation and culture

Murine mast cells (MCs) were obtained from C57BL/6(J) adult male and female mice aged 8-12 weeks. The inbred strain of C57BL mice was created in 1921 by C. C. Little at the Bussey Institute for Research in Applied Biology. Substrain 6 has been the most popular surviving substrain (Mekada, Abe et al. 2009).

2.2.1.1 Bone marrow-derived mast cells

Following euthanasia through cervical dislocation, the abdomen and legs of the mice were disinfected using 70 % ethanol. The skin around each leg, near the ileum, was incised, and subsequently removed by pulling it towards the feet. Then, the feet were disarticulated, and the femur and hip joint were exposed using sterile scissors and tweezers. The femur head was dislocated, and the leg was carefully cut without fracturing any bones. Any extraneous tissue was eliminated from the femur and tibia, which were then segregated, disinfected, and placed in a 50 ml tube containing wash medium, and maintained on ice. A sterile syringe with a needle and containing PBS was utilized to lavage the bone marrow. The bone marrow cells were pelletized through centrifugation at 300xg for 4-10 minutes at room temperature. The cells were then resuspended in culture medium (1 mouse per 15-20 ml medium) and the suspension was transferred into a tissue-treated cell culture flask, with the flask size selected based on the number of mice.

For the MC medium, RPMI medium supplemented with 10 % heat-inactivated fetal calf serum (FCS), 1 % penicillin/streptomycin solution (P/S), 1 % minimum essential medium (MEM), 1 % sodium pyruvate, 10 ng/ml murine IL-3, and stem cell factor (SCF) were added together. Cells were incubated at 37 ºC and 5 % CO2. Subsequently, the medium and flask were changed every two days until the cells attained the desired density, approximately 4-6 weeks into the cultivation process.

2.2.1.2 Mast cell degranulation assay and β-Hexosaminidase release measurement

All reagents used were pre-warmed at 37 °C. HEPES-Tyrodes buffer (1 ml/well) was added to the wall of a 12-well plate. The MCs were counted and diluted to 200,000 cells/well, followed by centrifugation (300xg for 3 minutes at RT) and discarding the buffer. The pellet was gently pipetted to resuspend it in 500 µl medium. IgE (1 µg/ml) was added to the cells and cultured for 1 hour (37 ºC, 5 % CO2). The plate was centrifuged (300xg for 3 minutes at RT), and the supernatant was discarded. DNP (0.01 µg/ml) was added and incubated for 1 hour at 37 ºC. Buffer was used as a control. The plate was centrifuged (300xg for 3 minutes at RT), and the supernatant and cell pellet were collected for further analysis.

To assess the degranulation of MCs, β-hexosaminidase release was measured by adding 50 µl supernatant from each condition (experiment and control group) to a 96-well black plate. Then,100 µl dH2O was added to all wells. The cells and plate were frozen at -80 °C for at least 30 minutes, after which the lysates and plate were thawed at 37 °C for at least 30 minutes. Fifty microliters of the obtained cell lysate from each well were transferred to the black plate. A 4-MUG dilution in citrate buffer (pH 4.5, 100 mM) was added to all wells. The plate was incubated for 1 hour at 37 °C, then covered with a lid to avoid evaporation, and finally 100 µl stop solution (Na-carbonate buffer, pH 10.7) was added to all wells. The optical density was analyzed in an ELISA reader (measuring fluorescence at 460 nm with excitation at 355 nm for 0.1 seconds), and the data were exported for analysis.

2.2.2 Cochlear tissue isolation

Postnatal day 3 to day 5 C57BL/6(J) mice were used to prepare cochlear organotypic cultures. The animals used were from the in-house breeding facilities of the Institute for

Experimental Medicine at the Charité Universitätsmedizin Berlin, and were ordered from and collected at the Charité Cross Over (CCO). To prevent the newborn animals from being cold, they were kept in a polystyrene box containing a previously heated gel pad. In addition, all mice received a subcutaneous injection of an electrolyte-dextrose mixture (0.04 ml per animal) to prevent dehydration.

The preparation of the cochlea was based on Sobkowicz et al. (1993) and Parker et al. (2010). Following decapitation, the head of the mouse was disinfected with 70 % ethanol and placed ventral side down. The scalp was removed, and the skull was cut along the mid-sagittal plane. The brain was removed carefully to expose the posterior fossa. The temporal bones were then separated from the posterior half of the skull and transferred into Petri dishes containing cold, sterile Dulbecco's Modified Eagle Medium/Nutrient Mixture F12 (DMEM/F12). Under a stereomicroscope, the tympanic membrane and annulus were carefully peeled away laterally, and the surrounding cartilage was removed to reveal the cochlear capsule. The cochlear capsules were then either broken off in small pieces from the oval window to the apex or extracted intact from the base. The stria vascularis (SV) and spiral ligament (SL) were detached as a single unit from the base to the apex, and the organ of Corti (OC) was separated from the modiolus. The OC explants were subsequently incubated in 4-well slides containing 500 µl of medium. The culture medium consisted of DMEM/F12, with 10 % fetal bovine serum, 1.3 % glucose, 0.2 % penicillin G, 0.2 % a solution of insulin, transferrin, and sodium selenite, and 0.025 % insulin-like growth factor. The culture medium was freshly prepared on the respective day of the experiment and sterilely filtered with a 0.2 µm syringe attachment.

OC explants were cultured using two distinct methods for subsequent analysis. For supernatant collection, whole OC tissues were incubated in a free-floating manner within the medium. For histological examination, the OC was laid flat at the bottom of the wells and secured in position by the surface tension of the culture medium. The explants were then incubated in the incubator (37 °C, 5 % CO2) for 24 hours pending further treatments.

2.2.3 Cochlear tissue treatment

2.2.3.1 Flat cochlear tissue explant treated with supernatant from IgE-anti-DNP/DNP stimulated BMMCs

Supernatants from the BMMCs degranulation assay described above were collected and prepared as aliquots for freezing at -80 °C. The supernatant was diluted in the OC medium with a total amount of 500 µl under sterile conditions daily during the experiment, as detailed in the Results section for the specific dilution factors. Controls were assigned to each treatment and cultured in a pure OC medium throughout the incubation period. The incubation was conducted at 37 °C with 5 % CO2 for 24 hours. The explants were fixed with 10 % formalin and stored in PBS at 4 °C until processing by immunofluorescence.

2.2.3.2 Stimulation of floating cochlear tissue with IgE-anti-DNP/DNP

All reagents were prepared under sterile conditions in a tissue culture hood and diluted in the 500 µl OC medium. The floating cochlear explants were first incubated with the mouse IgE- anti-DNP for 1 hour at 37°C with 5 % CO2, then stimulated with DNP for another 1 hour. The control groups assigned to each treatment condition were incubated in an OC medium over the entire incubation period. The supernatants were collected for further measurements.

2.2.3.3 Stimulation of floating cochlear tissue with compound 48/80

Compound 48/80 (CP48/80) was dissolved in distilled water and prepared as a stock solution at a concentration of 50 mM. It was then diluted in 500 µl OC medium to reach the working concentrations on each experiment day. Subsequently, the isolated free-floating OC explants were treated with CP48/80 for 1 hour. The control explants were cultured under the same tissue culture conditions in OC medium only at the end of the incubation period, and the supernatants were collected.

2.2.3.4 Exposure of floating cochlear tissue to cisplatin

Cisplatin was first dissolved in dimethyl sulfoxide (DSMO) to a final concentration of 100 mg/ml. Then, the dissolved cisplatin was diluted by a factor of 1:100 in DMEM/F12 medium and aliquoted. The concentration of the final stock solution was 3.3 mM. As specified

in the Results section, the explants were exposed to several concentrations of cisplatin for different periods. The control groups assigned to each treatment condition were incubated in the OC medium over the entire incubation period. The supernatants were collected for further measurements.

2.2.4 ELISA

The supernatants of BMMCs, as well as the supernatants of control or OC cultures treated with mouse IgE-anti-DNP/DNP, CP48/80, and cisplatin, were collected and used for the measurement of chymase, tryptase, and histamine by ELISA (Enzyme-linked immunosorbent assay). ELISAs were performed following the manufacturer's instructions.

2.2.4.1 Chymase measurement

The ELISA kit detecting mouse MC chymase 1 (CMA1) was used to measure chymase concentration in supernatants from degranulated BMMC and cochlear tissues. 100 µl of standard series and samples were prepared and added to wells pre-coated with a monoclonal antibody specific for mouse chymase and incubated at room temperature for 1 hour. The liquid from each well was aspirated without the washing step. 100 µl of detection reagent A working solution was then added to each well and the wells were covered with the plate sealer. The plate was incubated at 37 °C for 1 hour. Then, the solution was removed and the plate was washed with 350 µl of wash buffer 3 times with a multi-channel pipette. Next, the plate was gently patted on the absorbent paper to remove the remaining liquid. Then, 100 µl of detection reagent B working solution was added to each well, and the plate was covered with sealer and incubated for 30 minutes at 37 °C. The aspiration and wash step were repeated as conducted before 5 times. After the final wash in wash buffer, 90 µl of substrate solution was added to each well and incubated for 10-20 minutes (protected from light). Then, 50 µl of stop solution was added to each well. The plate was gently shaken to mix the liquid. The plate was then read immediately at 450 nm (reference absorbance 650 nm) using a SpectroMax M5 microplate reader (Molecular Devices).

2.2.4.2 Tryptase measurement

The ELISA kit detecting mouse MC tryptase (TPS) was used to measure tryptase concentration in supernatants from degranulated BMMC and cochlear tissues. 100 µl of

standard series and samples were prepared and added to wells pre-coated with a monoclonal antibody specific for mouse tryptase and incubated at room temperature for 1 hour. The liquid from each well was aspirated without the washing step. 100 µl of detection reagent A working solution was then added to each well and the wells were covered with the plate sealer. The plate was then incubated at 37 °C for 1 hour. The solution was removed, and the plate was washed with 350 µl of wash buffer 3 times with a multi-channel pipette. The plate was gently patted on the absorbent paper to remove the remaining liquid. Then, 100 µl of detection reagent B working solution was added to each well, the plate was covered with sealer and incubated for 30 minutes at 37 °C. The aspiration and wash step were repeated as conducted before 5 times. After the final wash in wash buffer, 90 µl of substrate solution was added to each well and incubated for 10-20 minutes (protected from light). Then, 50 µl of stop solution was added to each well. The plate was gently shaken to mix the liquid. The plate was then read immediately at 450 nm (reference absorbance 650 nm) using a SpectroMax M5 microplate reader (Molecular Devices).

2.2.4.3 Histamine measurement

The ELISA kit detecting histamine (HIS) was used to measure histamine concentration in supernatants from degranulated BMMC and cochlear tissues. 50 µl of the standard working solution of different concentrations was added to the first two columns. 50 µl of samples were also prepared and added to the appropriate wells. Immediately afterward, 50 µl of biotinylated detection antibody working solution was added to each well. The plate was then sealed with the provided cover and incubated at 37 °C for 45 min. Following incubation, the solution was removed from each well, and 350 µl of wash buffer was added. After letting it soak for 1-2 min, the solution was aspirated, and the plate was gently patted against absorbent paper to avoid remaining any liquid. The wash step was repeated 3 times. Subsequently, 100 µl of HRP Conjugate working solution was added to each well, the plate was resealed, and it was incubated for 30 minutes at 37 °C. The aspiration and wash steps were repeated as before, five times in total. After the final wash, 90 µl of substrate reagent was added to each well. The plate was covered with a new sealer and incubated for 10-20 min at 37 °C, protected from light. Then, 50 µl of stop solution was added to each well, and the contents were gently mixed by shaking the plate. The plate was read immediately at 450 nm (reference absorbance 650 nm) using a SpectroMax M5 microplate reader (Molecular Devices).

2.2.4.4 Multiple cytokine measurement

The ProcartaPlex™ Mouse Th1/Th2 Cytokine multiplex panel was used to measure the concentrations of multiple cytokines in supernatants from stimulated cochlear tissues. Capture bead mix was then added to the plate by vortexing the 1X capture bead mix vial for 30 seconds at high speed and adding 50 µl of the capture bead mix to each well using a multichannel pipette. The beads were washed using a hand-held magnetic plate washer by allowing them to settle for 2 minutes, removing the liquid, blotting the assembly to remove residual liquid, adding 150 µl of 1X wash buffer to each well, removing the liquid again, and blotting to ensure that no residual liquid remained. Samples and standards were subsequently added to the plate. For cell culture supernatants, 50 µl of prepared standards or samples were added per well, and 50 µl of cell culture medium was added to unused wells. The plate was sealed and shaken at 600 rpm for 60 minutes at room temperature and then stored at 4 °C overnight. The next day, the plate was washed three times, and subsequently, the biotinylated detection antibody mix was added to the plate, followed by incubation for 30 min at room temperature. After washing the plate 3 times, streptavidin-PE was added and incubated for 30 min at room temperature. Finally, the plate was prepared for analysis by adding 120 µl of reading buffer to each well. The samples were measured on a LuminexMAGPIX system and quantified using xPONENT analysis software (Luminex).

2.2.5 Fluorescent and immunofluorescent analyses

2.2.5.1 Hair cell quantification

Hair cell (HC) quantification was conducted for the flat cochlear tissue explants treated with supernatant from IgE-anti-DNP/DNP stimulated BMMCs. At the end of the incubation period, the flat OC explants were fixed in 10 % formalin solution for 45 minutes at room temperature and then washed 3 times with wash buffer. The fixation was conducted under a fume hood behind a protective glass. For the subsequent permeabilization, rinse buffer solution (0.5 % Triton X-100 in PBS) was added to the sample for 15 minutes at room temperature. To quantify the number and morphology of the HCs, the OC explants were stained with fluorescently labeled phalloidin. Phalloidin is the cyclic peptide toxin isolated from the green tuberous leaf fungus Amanita phalloides, which binds to filamentous actin (F-actin) with high affinity and inhibits its depolymerization (Wulf, Deboben et al. 1979).

Thus, phalloidin conjugated with the fluorescent dye can be used to visualize the filamentous actin-rich stereocilia and cuticular plates of the HCs using fluorescence microscopy. The HCs can be reliably distinguished based on their typical morphological arrangement in the OC and the stereocilia orientation. Phalloidin-iFluor® 594 was diluted by a factor of 1:1500 in PBS. The explants were then incubated at room temperature for 45 minutes, protected from light. After washing three times with wash buffer, the chamber of the 4-well slide was removed and the explants were embedded in ProLongTM gold antifading reagent containing DAPI. The explants were then covered with a cover slip and left at room temperature for a maximum of 24 hours to allow the mounting solution to dry. After that time, the slides were stored in a refrigerator at 4 °C.

The explants were imaged, quantified, and analyzed under the fluorescence microscopes EVOS FL and Keyence BZ-X800, under 40x magnification. Different filters were used to display the emission colours of the respective fluorochromes. The number of HC was counted along a 100 µm longitudinal segment in five distinct regions of each cochlear section. Intact HC was characterized by physiologically arranged stereocilia. Defective HC exhibited disturbed arrangements and/or fusions of the stereocilia. Cells were classified as missing when there were gaps in the typical arrays with no visible stereocilia or cuticular plate. An average value was calculated for each explant, with a minimum of five explants analyzed under each experimental condition.

2.2.6 Statistical analyses

The data were entered in Microsoft Excel® spreadsheets and then transferred to GraphPad Prism 9 software for statistical analysis. Statistical significance was calculated by a one-way ANOVA analysis with multiple comparisons using the Dunnett Test. The results of the descriptive statistics were presented as the mean ± SD (Standard deviation). A p-value ≤ 0.05 was considered statistically significant.

3. Results

3.1 Cochlear morphology changes after exposure to mouse IgE-anti-DNP/DNP-stimulated bone marrow-derived mast cell supernatant

To investigate the impact of mast cell (MC) degranulation on the morphology of the cochlea, the supernatant derived from bone marrow-derived mast cells (BMMCs) stimulated with mouse IgE-anti-DNP (1 µg/ml) and DNP (0.01 µg/ml) was collected. The supernatant was diluted to different concentrations according to several dilution factors (1:2000, 1:1000, 1:400, and 1:20) and incubated with the organ of Corti (OC) for 24 hours. Immunofluorescence staining of hair cells (HCs), as shown in Figure 2, revealed that the supernatant from activated MCs induces changes in cochlear architecture in a dose-dependent manner. Some HCs were missing, and the tissue appeared to be damaged. Analysis of the number of intact, damaged, and missing hair cells demonstrated a significant reduction in the numbers of viable outer hair cells (OHCs) and inner hair cells (IHCs) after treatment with MC supernatant compared to the control explants (Figure 3).

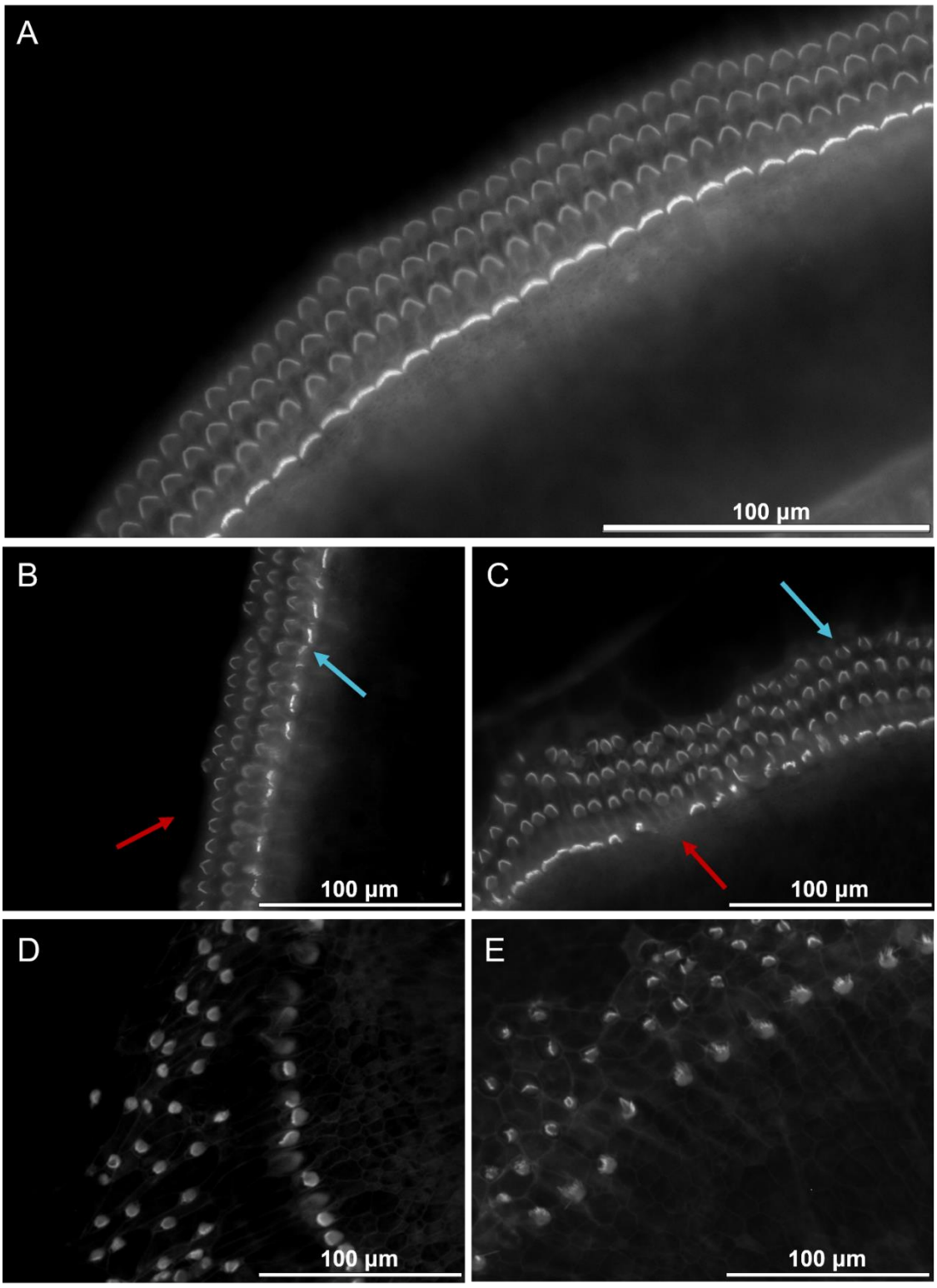

Figure 2. Morphological alterations in cochlear hair cells following incubation with BMMC degranulation supernatant. The representative epifluorescence micrographs of phalloidin-labeled HCs in OC cultures treated with different dilutions of BMMC supernatant are shown. Red arrowheads indicate representative missing cells and blue arrowheads indicate representative damaged cells. (A) Control group (n=12); (B) Treatment with 1:2000 dilution of MC supernatant (n=13); (C) Treatment with 1:1000 dilution of MC supernatant (n=7); (D) Treatment with 1:400 dilution of MC supernatant (n=11); (E) Treatment with 1:20 dilution of MC supernatant (n=10); The scale bar is shown.

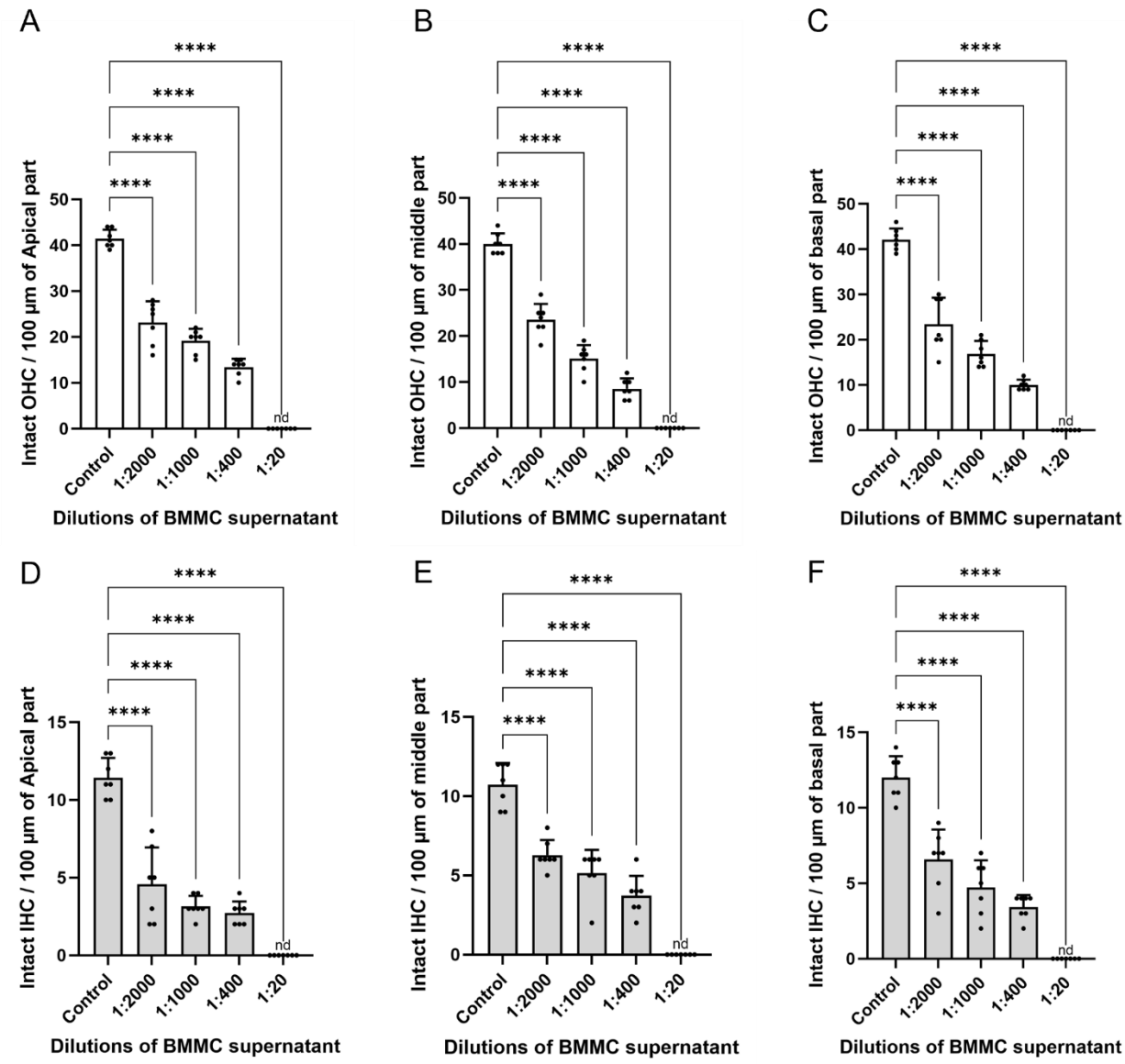

Figure 3. Hair cell loss caused by BMMC supernatant. The number of intact OHC per 100 µm length at the apical (Fig. 3A), middle (Fig. 3B), and basal parts of the cochlea (Fig. 3C), as well as the number of intact IHC per 100 µm length at the apical (Fig. 3D), middle (Fig. 3E), and basal (Fig. 3F) parts of OC explants, were significantly reduced by incubation with MC supernatant. Data is from 7 separate experiments. Bars represent mean ± SD. * $p < 0.05$; ** $p < 0.01$; *** $p < 0.001$; **** $p < 0.0001$ (one-way ANOVA).

3.2 Stimulation with mouse IgE-anti-DNP/DNP does not result in the release of chymase and tryptase from cochlear explants.

To examine whether cochlear explants respond to stimulation with mouse IgE-anti-DNP/DNP, the OC explants were first isolated and sensitized with various concentrations of mouse IgE-anti-DNP for 1 hour, followed by an additional hour of various concentrations of DNP stimulation. Subsequently, the supernatants were collected for ELISA analysis. Chymase and tryptase, two key enzymes of MC, were selected as the target factors for this experiment. The experimental groups consisted of five concentrations: 0.1-1 µg/ml mouse IgE-anti-DNP and 0.01-0.1 µg/ml DNP, while the control group received culture medium alone. As shown in Figure 4, when compared to the control group, no significant chymase or tryptase was detected in the supernatants collected from OC cochlear explants stimulated with mouse IgE-anti-DNP/DNP ($p > 0.05$; one-way ANOVA).

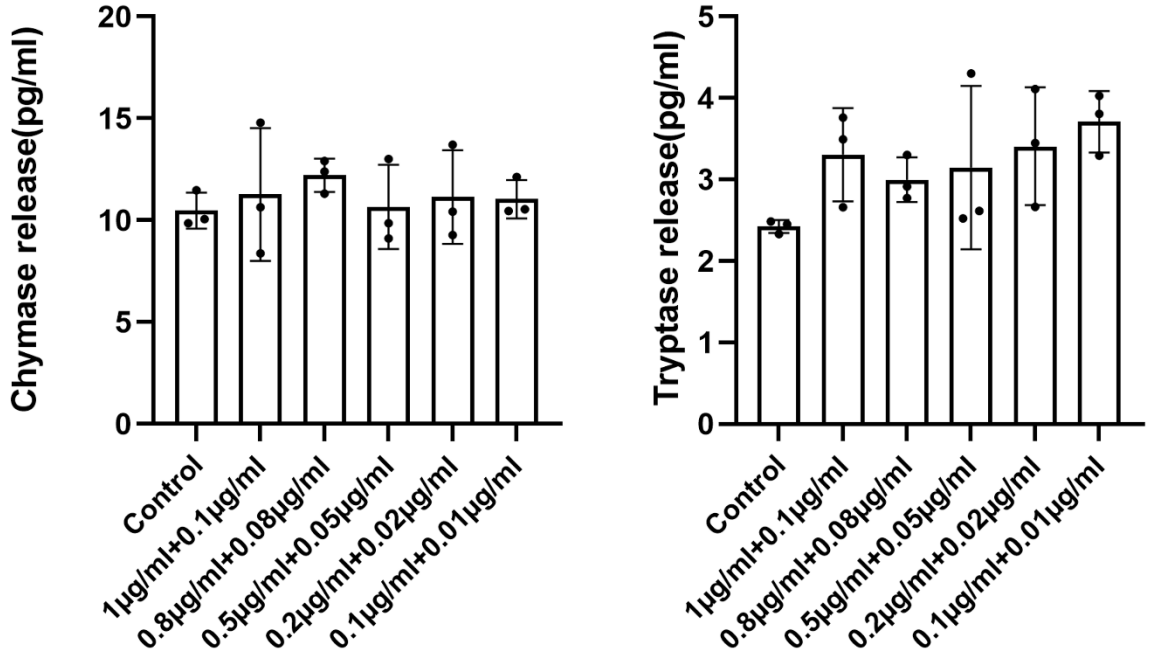

Figure 4. Chymase and tryptase release from murine cochlear explants evoked by mouse IgE-anti-DNP/DNP. The cochlear explants were incubated with the mouse IgE-anti-DNP compound at different concentrations for 1 hour at 37 °C, then stimulated with DNP (0.01- 0.1 µg/ml) also for 1 hour. The horizontal axis indicates IgE-anti-DNP (0.1-1 µg/ml) + DNP (0.01-0.1 µg/ml). No significant release of chymase and tryptase was detected in the experiment groups. Data are from 3 separate experiments. Bars represent mean ± SD (one-way ANOVA).

3.3 Compound 48/80 stimulates the release of chymase and tryptase from cochlear explants.

As described above, the activation of MCs can be defined as FcεRI (the high-affinity IgE receptor)-dependent and FcεRI-independent. Compound 48/80 (CP48/80) is a polymer that can bind to the G-protein-coupled receptor, initiating activation signals that result in an elevated intracellular Ca^{2+} concentration in MCs, thereby triggering degranulation in an FcεRI-independent way (Palomäki and Laitinen 2006, Kashem, Subramanian et al. 2011).

To examine whether resident MCs in cochlear explants respond to stimulation with CP48/80, the OC explants were exposed to CP48/80 (20 µM, 50 µM, and 100 µM) for 30 minutes. The control group was left in a pure OC culture medium. Subsequently, the supernatants were collected for ELISA analysis. Compared to the control group, a significant release of tryptase and chymase was detected in the supernatants collected from OC explants stimulated with CP48/80 in a dose-dependent manner (Figure 5).

Compared to the control group, all experimental groups exhibited significant chymase release (in the 20 µM group, 3.56 vs 18.71 pg/ml, $p=0.0021$; in the 50 µM group, 3.56 vs 40.14 pg/ml, $p<0.0001$; in the 100 µM group, 3.56 vs 51.60 pg/ml, $p<0.0001$). However, significant increases in tryptase were observed only by simulation with 50 µM (7.77 vs 11.4 pg/ml, $p=0.0014$) and 100 µM (7.77 vs 10.27 pg/ml, $p=0.0212$) of CP48/80, whereas CP48/80 used at 20 µM showed no significance (7.77 vs 8.76 pg/ml, $p>0.05$).

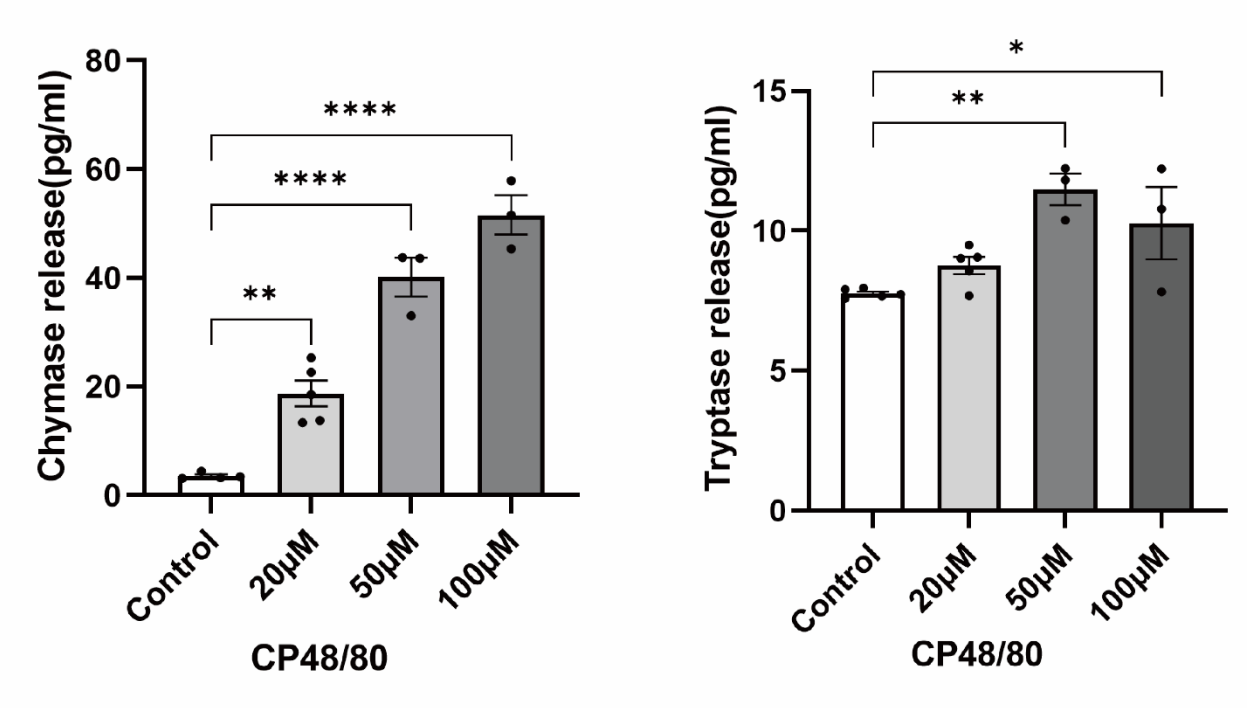

Figure 5. Chymase and tryptase release from whole cochlear explants treated with CP48/80 for 30 min. The experiment groups were exposed to 20 μM (n=5), 50 μM (n=3), and 100 μM (n=3) of CP48/80 for 30 min, and cochlear explants with medium only were used as control groups (n=4). Bars represent mean ± SD. **** $p < 0.001$, *** $p < 0.005$, ** $p < 0.01$, * $p< 0.05$ (one-way ANOVA).

Considering the distribution of MCs in the membranous cochlea (Karayay, Olze et al. 2023), the cochlear tissue was also partitioned into two distinct regions, the spiral limbus (with OC) and the lateral wall, including the stria vascularis (SV) and spiral ligament (SL), to assess their respective responses to CP48/80. To ensure that a measurable response was obtained in each distinct region, a longer exposure time was used for the partitioned cochlear tissues in this experiment. After isolation, each sample was cultured with CP48/80 for 90 min, and the ones cultured with medium only served as the control group. The supernatants were collected for ELISA. Upon stimulation with CP48/80, both chymase and tryptase were detected in the supernatant from spiral limbus (Figure 6) and lateral wall (Figure 7) in a dose-dependent manner.

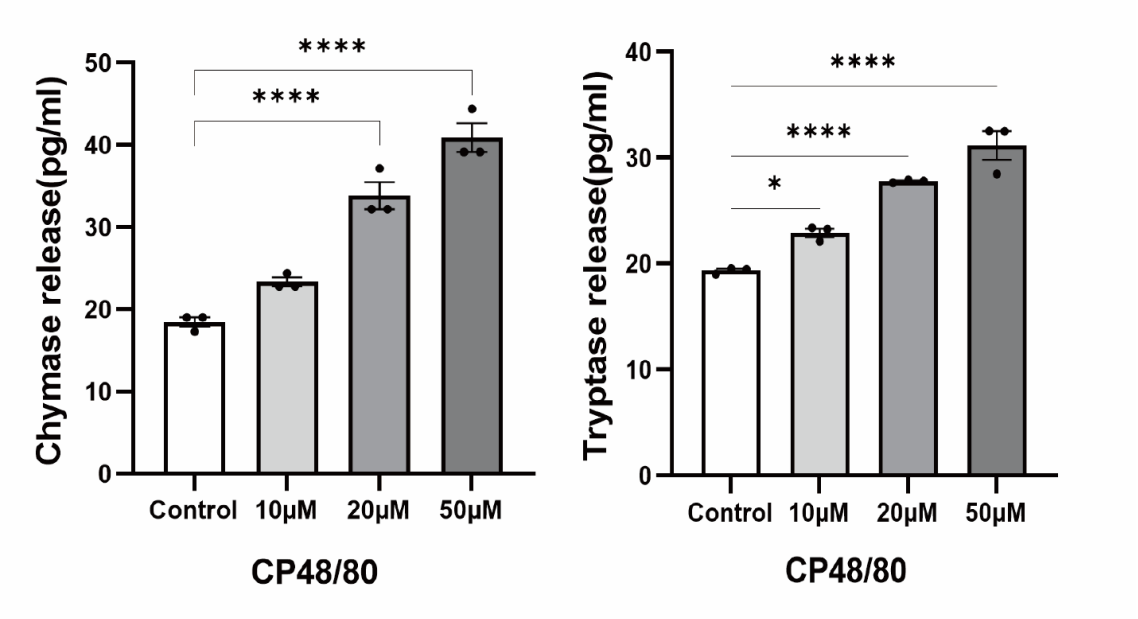

Figure 6. Chymase and tryptase release from spiral limbus treated with CP48/80 for 90 min. The spiral limbus containing the organ of Corti (OC) was isolated from the cochlear tissue. Experiment groups were exposed to 10 µM, 20 µM, and 50µM of CP48/80 for 90 min, and spiral limbus (with OC) treated with medium only was used as the control group. The data shown in the figure are from 3 separate experiments. Bars represent mean ±SD. **** $p < 0.001$, * $p < 0.05$ (one-way ANOVA).

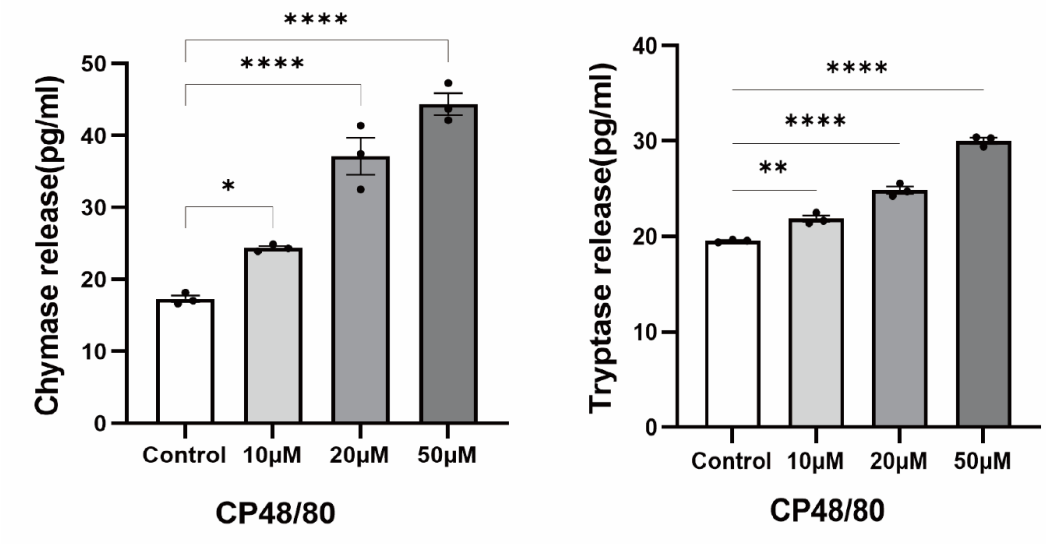

Figure 7. Chymase and tryptase release from lateral wall treated with CP48/80 for 90 min. Cochlear lateral wall (LW) explants containing the stria vascularis (SV) and spiral ligament (SL) were isolated from the cochlear tissue. Experiment groups were exposed to 10 µM, 20 µM, and 50 µM of CP48/80 for 90 min and LW treated with medium only was used as the control group. The data shown are means from 3 separate experiments. Bars represent mean ± SD. **** $p < 0.001$, ** $p < 0.01$, * $p < 0.05$ (one-way ANOVA).

3.4 Immediate effects of cochlear explant exposure to cisplatin on the release of cytokines, histamine, chymase, and tryptase

3.4.1 Lack of release of chymase or histamine by cisplatin from individual floating cochlear explants

The response of cochlear tissue to cisplatin stimulation was also studied. At the onset of the experiment, a single cochlear tissue specimen was included in each sample. The cochlea was freshly isolated and exposed to different concentrations of cisplatin for a duration of 1 hour. Cochlear tissues treated solely with OC medium served as the control group. Supernatants were subsequently collected to quantify the levels of chymase and histamine by ELISA. No statistically significant release of chymase or histamine was observed across the various experimental groups when compared to the control group (Figure 8).

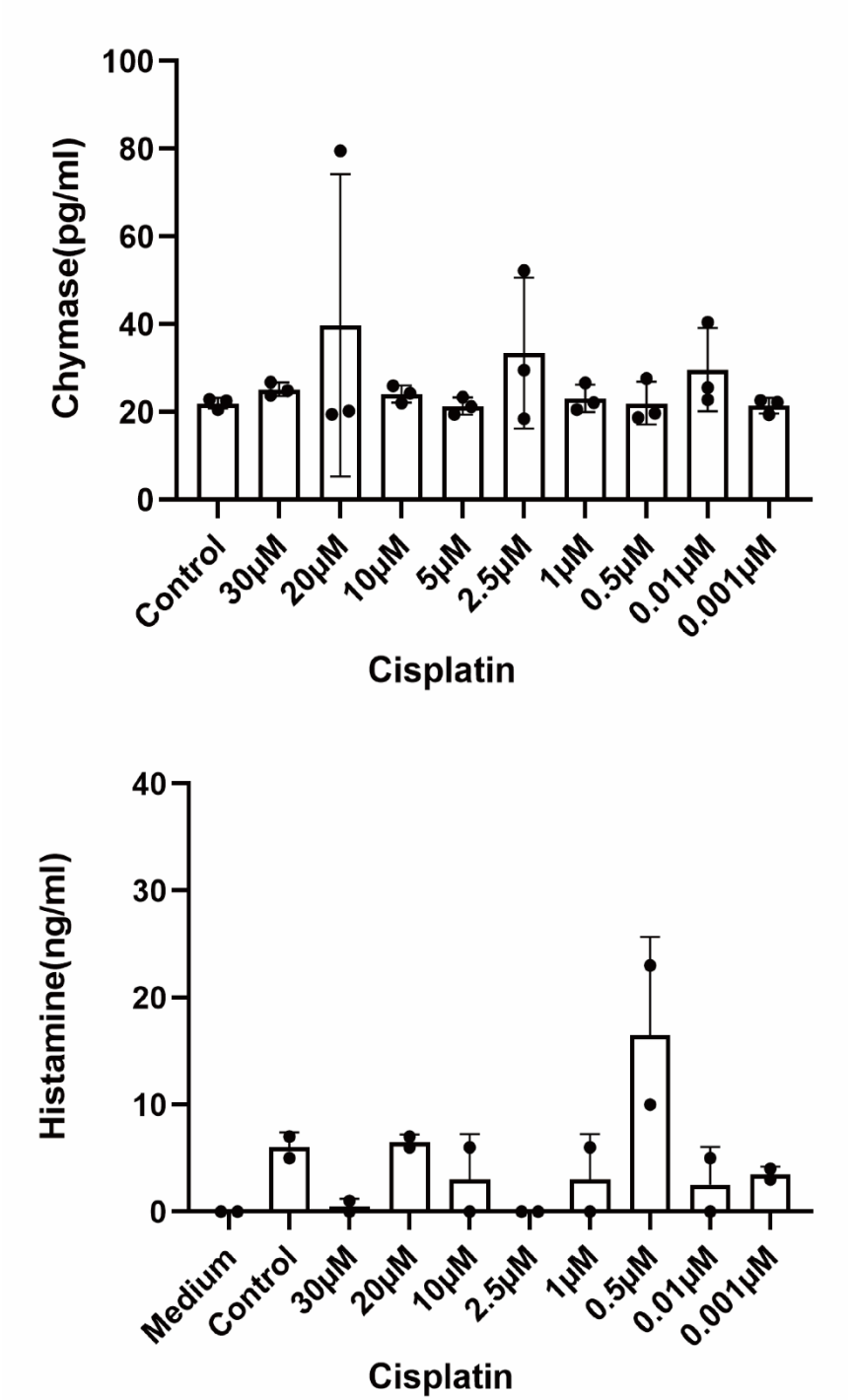

Figure 8. The effect of cisplatin exposure on cytokine release from individually cultured cochlear explants. Single cochlear explants were incubated with the cisplatin compound at different concentrations for 1 hour at 37 °C. No significant release of chymase and histamine was observed under the experimental conditions. Data show means from 3 separate experiments. Bars represent mean ± SD (one-way ANOVA).

3.4.2 Cisplatin induces the release of GM-CSF, TNF, IFNy, IL-6, and IL-18 upon simultaneous stimulation of four cochlear explants in one tissue culture well

Based on the data above, adjustments were made. Instead of one, four cochlear tissues were placed in each dish for subsequent trials. The experiment was reiterated, with concentrations of cisplatin at 0.5 µM, 10 µM, 15 µM, and 30 µM. Following a 1-hour incubation period, the supernatant was collected for cytokine analysis. Significant release of certain cytokines was observed in the experimental group treated with cisplatin at a concentration of 15 µM (Figure 9). Specifically, elevated levels of GM-CSF (3.19 vs 8.65 pg/ml, p=0.0029), TNF-alpha (3.66 vs 23.30 pg/ml, p=0.0011), IFNy (2.18 vs 10.60 pg/ml, p=0.0076), IL-6 (5.52 vs 793.7 pg/ml, p=0.0018), and IL-18 (35.57 vs 1562 pg/ml, p=0.0009) were detected compared to the control group.

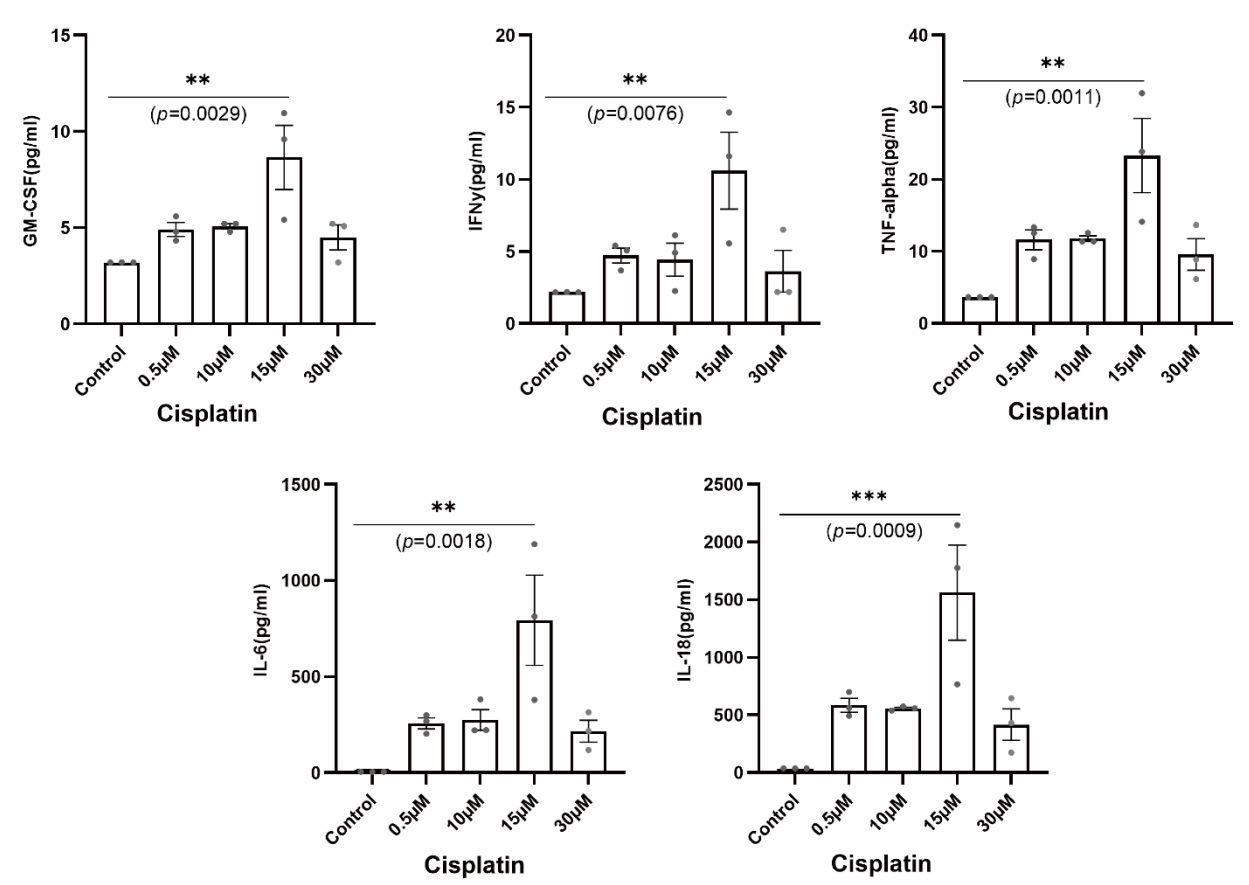

Figure 9. Cisplatin induces the release of GM-CSF, IFNy, TNF, IL-6, and IL-18 from cochlear explants. The cochlear explants were incubated with the cisplatin compound at various concentrations (0.5 µM, 10 µM, 15 µM, and 30 µM) at 37 °C for 1 hour. Significant release of GM-CSF, IFNy, IL-6, IL-18, and TNF-alpha was detected in the supernatants in the 15 µM cisplatin group. The data shown are means from 3 separate experiments. Bars represent mean ± SD. **** p < 0.001, *** p < 0.005, ** p < 0.01 (one-way ANOVA).

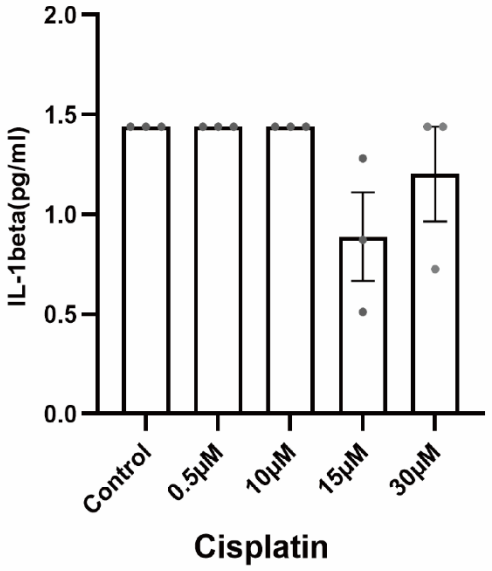
IL-1beta(pg/ml)
2.0
1.5
1.0
0.5
0.0
Control
0.5μM
10μM
15μM
30μM
Cisplatin

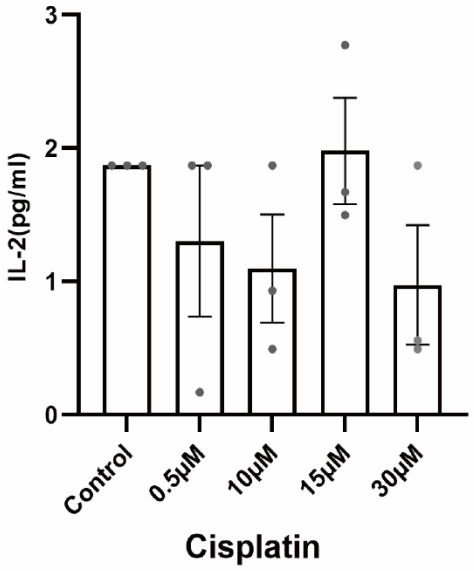
IL-2(pg/ml)
3
2
1
0
Control
0.5μM
10μM
15μM
30μM
Cisplatin

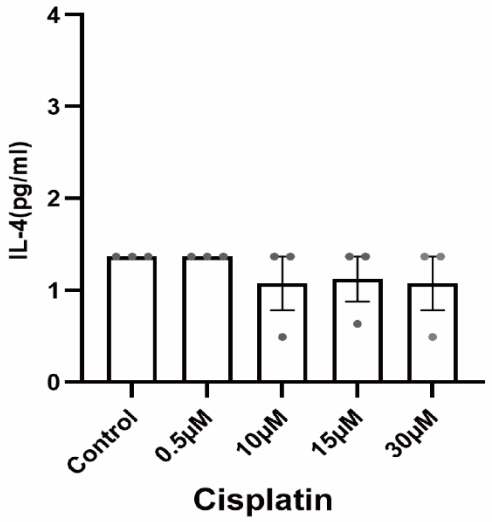
IL-4(pg/ml)
4
3
2
1
0
Control
0.5μM
10μM
15μM
30μM
Cisplatin

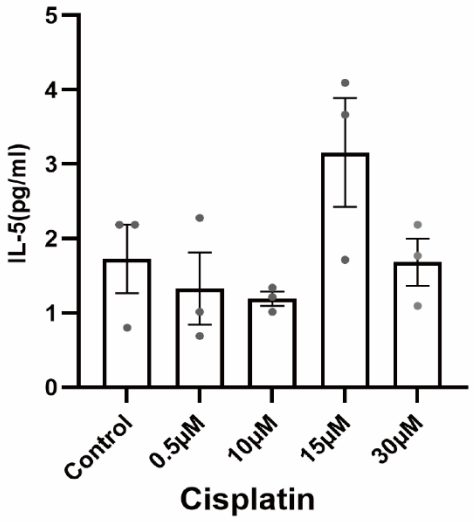
IL-5(pg/ml)
5
4
3
2
1
0
Control
0.5μM
10μM
15μM
30μM
Cisplatin

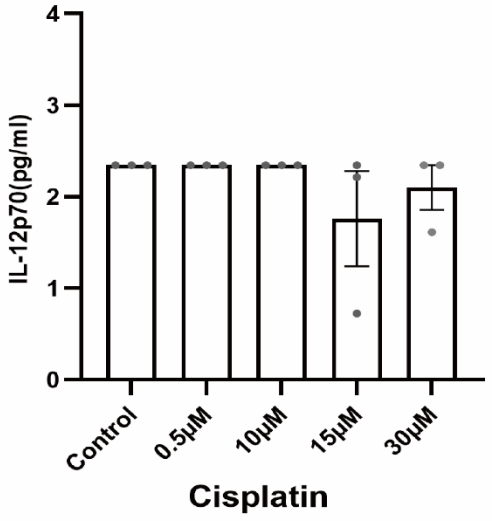
IL-12p70(pg/ml)
4
3
2
1
0
Control
0.5μM
10μM
15μM
30μM
Cisplatin

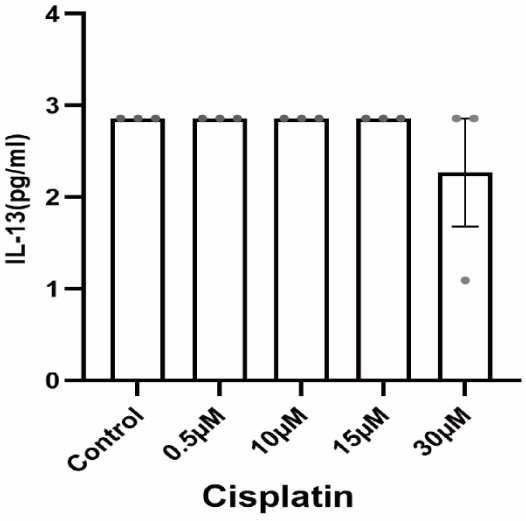
IL-13(pg/ml)
4
3
2
1
0
Control
0.5μM
10μM
15μM
30μM
Cisplatin

Figure 10. Cisplatin fails to induce the release of IL-1beta, IL-2, IL-4, IL-5, IL-12p70, and IL-13 release from cochlear explants. The cochlear explants were incubated with the cisplatin compound at various concentrations (0.5 µM, 10 µM, 15 µM, and 30 µM) at 37 °C for 1 hour. Statistically significant releases of IL-1beta, IL-2, IL-4, IL-5, IL-12p70, and IL-13 were not detected in the supernatants of the experimental group. The data shown are from 3 separate experiments. Bars represent mean ± SD. (one-way ANOVA).

3.4.3 Time course of histamine and tryptase release from cochlear explants exposed to 15 µM of cisplatin

Based on the data above, the cochlear explants were incubated with 15 µM cisplatin at various times. Supernatants were collected to measure key mediators of MCs, histamine, tryptase and chymase. As shown in Figure 11, histamine was detected in the supernatants of OC explants after 1 hour of cisplatin stimulation (1 vs 1.8 ng/ml, $p<0.0001$) and remained stable within 24 hours of incubation (1 vs 1.7 ng/ml, $p<0.0001$). A significant release of tryptase. was found when the experiment explants were cultured with cisplatin compound for 2 hours (0.6 vs 0.9 pg/ml, $p=0.0191$). In the same supernatants, no chymase was found.

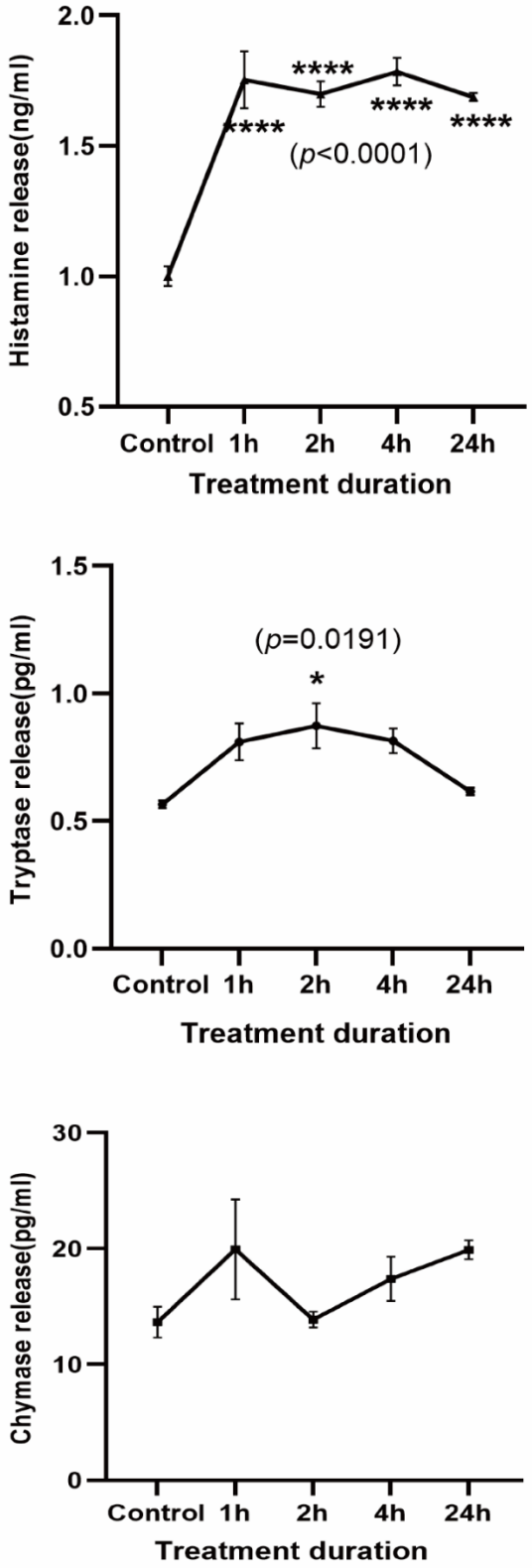

Figure 11. Time course for histamine, tryptase, and chymase release from cochlear explants evoked by cisplatin. The cochlear explants were incubated with the cisplatin compound at 15 µM at various times at 37 °C. The data are the means from 3 separate experiments. Bars represent mean ±SD. **** $p < 0.001$, * $p < 0.05$ (one-way ANOVA).

4. Discussion

4.1 Mast cells in the inner ear

Mast cells (MCs) are crucial immune cells, and since their description and naming by Paul Ehrlich in 1878, they have gathered considerable interest from researchers worldwide. Mature MCs are distributed in various tissues, including the dermis (Eady, Cowen et al. 1979), pulmonary alveoli and respiratory tract (Schulman, MacGlashan et al. 1982), intestinal mucosa (Strobel, Miller et al. 1981), conjunctiva (Irani, Butrus et al. 1990), as well as the atrial appendages of the heart (Sperr, Bankl et al. 1994), among others. However, it wasn't until 2020 that the presence of MCs in the inner ear of rodents was first discovered and confirmed by the ENT research laboratory at the Charité Universitätsmedizin Berlin (Szczepek, Dudnik et al. 2020). Subsequent investigations persistently revealed that MCs in the cochlea exhibited degranulation following cisplatin treatment, and that the application of the MC stabilizer cromolyn conferred protective effects against cisplatin-induced damage to hair cells (HCs) and spiral ganglion neurons (SGN) (Karayay, Olze et al. 2023), indicating the involvement of resident cochlear MCs in the pathological processes induced by cisplatin in the cochlea. Yet the exact mechanism remains unknown.
The primary objective of this study was to investigate the impact of degranulated MCs on cochlear morphology. Subsequently, the study delved into elucidating the capacity for the activation of MCs residing in the cochlea in response to various stimuli. Finally, this investigation provided preliminary insights into the mechanisms through which MCs contribute to the ototoxic effects of cisplatin.

4.2 Effect of mast cell degranulation on cochlear morphology

Epidemiological evidence has indicated a clinical correlation between allergic diseases and inner ear dysfunction (Derebery and Berliner 2000, Derebery and Berliner 2010, Banks, McGinness et al. 2012, Zeng, Domarecka et al. 2024). To simulate type 1 hypersensitivity reaction in this *in vitro* experiment, bone marrow-derived mast cell (BMMC), and mouse IgE-anti-DNP/DNP were employed as a pathological model to induce MC degranulation following antigenic stimulation via an IgE-dependent pathway. BMMCs were initially isolated from adult C57/BL6 mice and subsequently cultured for 4-6 weeks to attain the desired density level. Degranulation assays were then conducted on mature

BMMCs. After stimulation of BMMCs with IgE-anti-DNP and DNP, the collected supernatants containing MC-derived mediators were diluted using various dilution factors and subsequently co-cultured with isolated cochlear explants for 24 hours. Subsequent fluorescence staining and HC counting revealed that degranulated BMMC supernatant exerted detrimental effects on cochlear morphology. As the concentration of the supernatant increased, the initial orderly arrangement of HCs became disrupted, and the number of intact cells decreased.

These findings underscore the potential link between allergic diseases, MC activation, and hearing loss. Allergic responses involving MC degranulation release various mediators, such as histamine, cytokines, and proteases (chymase and tryptase, etc.), which can induce inflammation and tissue damage (Metcalfe, Baram et al. 1997, Metz and Maurer 2007). In the inner ear, where delicate structures like HCs are crucial for auditory function, any disruption in morphology can have significant consequences on hearing.

4.3 Effect of mouse IgE-anti-DNP/DNP on cochlear mast cells

In the second phase of this study, the direct impact of mouse IgE-anti-DNP and DNP on resident cochlear MCs was investigated, aiming to elucidate the potential involvement of resident cochlear MCs in allergic response within the inner ear. Following isolation, the cochlear explants of p3-5 days old C56/BL6 mice were initially incubated with mouse IgE-anti-DNP for one hour, utilizing a concentration gradient ranging from 0.1 µg/ml to 1 µg/ml. Subsequently, DNP stimulation was conducted for one hour, employing concentrations ranging from 0.01 µg/ml to 0.1 µg/ml. The supernatants were then collected for chymase and tryptase measurements. Interestingly, despite the range of concentrations tested, no significant release of chymase and tryptase, two key proteases associated with MC activation, was observed under the experimental conditions.

This result indicated that the IgE-anti-DNP and DNP stimulation could not induce the degranulation of cochlear resident MCs under the experimental conditions of the study.

Potential explanations are as follows: 1. Experimental concentration: according to previous experimental protocols established by our laboratory, degranulation experiments involving BMMC utilize a concentration of 1 µg/ml of mouse IgE-anti-IgE and 0.1 µg/ml of DNP per 20,000 MCs. Given the limited number of MCs present in each newborn mouse cochlea (Karayay, Olze et al. 2023), the concentrations of mouse IgE-anti-DNP and DNP

were adjusted accordingly, and concentration gradient experiments were conducted. Nevertheless, it remains plausible that the chosen concentrations were not optimal for stimulating cochlear MCs, resulting in non-significant outcomes. 2. Limited cell quantity: the limited number of MCs in the inner ear may not be sufficient to produce discernible differences in the supernatant even if the MCs are successfully activated and degranulated. 3. Molecular weight barrier: the high molecular weights of mouse IgE-anti-DNP and DNP may have hindered their effective penetration into the cochlear tissue, thereby impeding their ability to stimulate resident cochlear MCs *in vitro*. 4. Differential activation mechanisms: it is conceivable that there are disparities in the activation mechanisms or mediator responses of resident cochlear MCs compared to BMMCs. The unique microenvironment of the cochlea could potentially influence MC behaviour, leading to disparate responses to allergenic stimuli. 5. IgE binding occupancy: it is plausible that cochlear MCs in the inner ear had already bound to IgE, rendering them unable to bind to the mouse IgE-anti-DNP utilized in this study. Future experiments should consider employing anti-IgE instead of DNP.

4.4 Effect of compound 48/80 stimulation on cochlear mast cells

CP48/80 functions as a classical MC activator by inducing MC degranulation through its interaction with the Mrgprb2 receptor located on MC membranes (Ferry, Brehin et al. 2002). Mrgprb2 (the murine direct homolog of human MRGPRX2) or MRGPRX2 are receptors primarily investigated in the context of non-IgE-mediated MC degranulation and inflammation (Ferry, Brehin et al. 2002, Tatemoto, Nozaki et al. 2006, Baldo 2023). Stimulation of Mrgprb2 and MRGPRX2 with neuropeptides (e.g. Substance P) and other polybasic secretagogues (e.g. CP48/80) leads to IgE-independent anaphylactic reactions (Ferry, Brehin et al. 2002, McNeil, Pundir et al. 2015, Ogasawara, Furuno et al. 2019). The third research objective of this study was to evaluate the responsiveness of resident cochlear MCs to CP48/80 stimulation. The results depicted in Figure 5 revealed significant chymase release at varying concentrations (20 µM, 50 µM, and 100 µM), along with tryptase release observed only in the 50 µM and 100 µM experimental groups. Additionally, both chymase and tryptase were detected following separate stimulation of the lateral wall (containing spiral ligament and stria vascularis) and spiral limbus (containing the organ of Corti) with CP48/80 (Figures 6-7). It is noteworthy that the incubation period for

stimulating the entire cochlea was 1 hour, while the incubation period for separately stimulating the lateral wall and spiral limbus was extended to 90 minutes. This discrepancy in incubation times may account for the potential inability of the experimental timeframe to capture the release of tryptase by the 20 µM CP48/80 in the whole cochlear tissue experiment, resulting in an apparent lack of significance in the 20 µM concentration experimental outcomes (Figure 5).

4.5 The effect of cisplatin on cochlear mast cells

The investigation into the impact of cisplatin on cochlear resident MCs represents a significant aspect of this study, particularly concerning its relevance to ototoxicity and potential implications for hearing loss. Cisplatin, a frequently utilized chemotherapeutic agent, is recognized for its potential to induce cochlear damage and subsequent hearing loss (Rybak 2007, Brock, Knight et al. 2012). However, the intricate and specific mechanisms underlying these effects remain incompletely elucidated. This study postulates that MCs located in the cochlea may contribute to the pathological processes associated with cisplatin-induced ototoxicity.

Initially, individual floating cochlear tissue was placed in each culture dish for cisplatin stimulation experiments. However, neither histamine nor chymase was detected in the supernatant.

This contrasts with the previous report from the Charité HNO laboratory indicating degranulation of resident MCs in response to cisplatin stimulation (Karayay, Olze et al. 2023). It is important to note that the previous study utilized fluorescent staining techniques to visualize individual MCs, whereas our approach focused on the analysis of supernatants after tissue culture, which may have made the detection of MC mediators challenging. In response to these initial findings, and taking into account the limited number of MCs in each cochlea (Karayay, Olze et al. 2023), modifications were made to the experimental setup. The number of cochlear tissues in each dish was increased to enhance the sensitivity of the assay. Subsequent experiments, using selective concentrations of cisplatin stimulation, revealed elevated levels of various cytokines, including GM-CSF, IFNy, IL-6, IL-18, and TNF, upon 15 µM cisplatin stimulation. These findings imply an immediate inflammatory reaction within the cochlea following exposure to cisplatin, with resident MCs potentially playing a role in the release of cytokines. This underscores the

importance of conducting further investigations in the future to delve deeper into this phenomenon.

Furthermore, time-course experiments conducted with 15 µM cisplatin revealed a time-dependent release of histamine and tryptase, particularly histamine, which exhibited a steady release from 1 hour to 24 hours. This pattern suggests an activation response of resident cochlear MCs to cisplatin, which is also consistent with the findings of Brzezińska-Błaszczyk et al. (Brzezińska-Błaszczyk, Mińcikiewicz et al. 1996). Their study demonstrated that peritoneal cavity-derived MCs degranulate to secrete histamine in the presence of cisplatin. However, chymase release was not observed under our experimental conditions. This observation implies that cisplatin might selectively influence the release of some MC mediators within the cochlea, and that the chymase in the cochlea may display a distinct response compared to histamine and tryptase. Nonetheless, further detailed investigations would be necessary to confirm this assumption.

Several factors may contribute to the observed differences in MC mediator release in response to cisplatin stimulation. The specific mechanisms underlying MC activation by cisplatin, including receptor interactions and intracellular signalling pathways, warrant further investigation. Additionally, the microenvironment within the cochlea, including the presence of other immune cells, cytokines, and growth factors, may influence MC responsiveness to cisplatin. Overall, the findings from this study shed light on the complex interplay between cisplatin exposure, cochlear resident MCs, and inflammatory responses within the inner ear. Further study is necessary to clarify the precise mechanism by which cisplatin modulates MC function as well as its implications for cisplatin-induced ototoxicity and hearing loss. Understanding these mechanisms may offer new avenues for mitigating the adverse effects of cisplatin on auditory function and improving the management of chemotherapy-induced hearing loss.

4.6 Limitations and future directions

The limitations of the current study primarily come from the research methodology employed. Firstly, in the initial phase of the study, where degranulated BMMC supernatant was utilized to induce cochlear morphological damage, pinpointing the specific mediators responsible for the damage proved challenging. MC degranulation results in the secretion of a diverse array of mediators, including histamine, serotonin, chymase, tryptase, and

various cytokines, leading to a complex interplay of “cocktail” effects. Secondly, the lack of an established effective method for isolating MCs from the inner ear presented a significant limitation. As a result, all the experimental outcomes only indirectly reflect the function of cochlear MCs in physiological and pathological processes, making it difficult to directly ascertain the role of cochlear MCs.

Future investigations are warranted to unravel the precise mediators and signalling cascades implicated in MC-mediated cochlear damage. Employing an MC stabilizer, such as cromoglicic acid, could represent a potential strategy to comprehensively identify the spectrum of mediators contributing to cisplatin-induced ototoxicity. By delineating the disappearing mediators, this approach lays the groundwork for subsequent studies delving into the underlying signalling pathways, thus advancing our comprehension of cisplatin-induced ototoxicity and paving the way for developing innovative therapeutic interventions.

5. Conclusions

At the end of the dissertation, I will summarize this research as follows. The results of this study answer the research question posed at the beginning: Cochlear morphology in murine, especially auditory receptor hair cells (HCs), was significantly affected by degranulated mast cells (MCs), shedding light on a potential mechanistic link between inner ear disorders and MC-driven conditions. Clinical investigations examining hearing loss prevalence in individuals with allergic disorders could offer valuable epidemiological insights corroborating this association. Moreover, the observed responsiveness and functionality of resident cochlea MCs to stimulation with Compound 48/80, even when present in limited numbers, underscores their sensitivity and viability within the inner ear milieu. The activation of resident cochlear MCs led to the release of various mediators, including histamine, tryptase, and a range of cytokines, in response to cisplatin stimulation. These findings are supported by previous research conducted at the Otolaryngology Research Laboratory at the Charité Medical University in Berlin, demonstrating the protective effects of the MC stabilizing agent cromoglicic acid against cisplatin-induced HC loss and neurotoxicity. This suggests that resident cochlear MCs are likely to play a role in cisplatin-induced ototoxicity, and the pathological effects initiated by MCs may even precede the accumulation of ROS induced by cisplatin. However, further investigation into the specific molecular pathways involved is necessary. The present study provides a solid foundation for future research aimed at developing therapeutic interventions for treating cisplatin-induced hearing loss by examining mediator release and biochemical processes in greater detail.

Overall, this study underscores the intricate nature of MC biology and its significance in the immune response of the inner ear. While MCs are well-recognized in allergic diseases and inflammation, their specific involvement in cochlear pathology warrants continued exploration.

Reference list

Abraham, S. N. and A. L. St John (2010). "Mast cell-orchestrated immunity to pathogens." Nat Rev Immunol **10**(6): 440-452.

Altoè, A., V. Pulkki and S. Verhulst (2018). "The effects of the activation of the inner-hair-cell basolateral K(+) channels on auditory nerve responses." Hear Res **364**: 68-80.

Baldo, B. A. (2023). "MRGPRX2, drug pseudoallergies, inflammatory diseases, mechanisms and distinguishing MRGPRX2- and IgE/FcεRI-mediated events." Br J Clin Pharmacol **89**(11): 3232-3246.

Banks, C., S. McGinness, R. Harvey and R. Sacks (2012). "Is allergy related to Meniere's disease?" Curr Allergy Asthma Rep **12**(3): 255-260.

Bohn, A. and W. König (1982). "Generation of monoclonal DNP-specific IgM and IgE murine antibodies on the efficacy of hybridization." Mol Immunol **19**(2): 193-199.

Bohn, A. and W. König (1982). "Generation of monoclonal murine anti-DNP-IgE, IgM and IgG1 antibodies: biochemical and biological characterization." Immunology **47**(2): 297-311.

Bosher, S. K. and R. L. Warren (1968). "Observations on the electrochemistry of the cochlear endolymph of the rat: a quantitative study of its electrical potential and ionic composition as determined by means of flame spectrophotometry." Proc R Soc Lond B Biol Sci **171**(1023): 227-247.

Boyce, J. A. (2003). "The role of mast cells in asthma." Prostaglandins Leukot Essent Fatty Acids **69**(2-3): 195-205.

Braun, K., F. Böhnke and T. Stark (2012). "Three-dimensional representation of the human cochlea using micro-computed tomography data: presenting an anatomical model for further numerical calculations." Acta Otolaryngol **132**(6): 603-613.

Brock, P. R., K. R. Knight, D. R. Freyer, K. C. Campbell, P. S. Steyger, B. W. Blakley, S. R. Rassekh, K. W. Chang, B. J. Fligor, K. Rajput, M. Sullivan and E. A. Neuwelt (2012). "Platinum-induced ototoxicity in children: a consensus review on mechanisms, predisposition, and protection, including a new International Society of Pediatric Oncology Boston ototoxicity scale." J Clin Oncol **30**(19): 2408-2417.

Brzezińska-Błaszczyk, E., M. Mińcikiewicz and J. Ochocki (1996). "Effect of cisplatin and cis-platinum (II) phosphonate complex on murine mast cells." Eur J Pharmacol **298**(2): 155-158.

Chen, C. C., M. A. Grimbaldeston, M. Tsai, I. L. Weissman and S. J. Galli (2005). "Identification of mast cell progenitors in adult mice." Proc Natl Acad Sci U S A **102**(32): 11408-11413.

Church, M. K., P. Kolkhir, M. Metz and M. Maurer (2018). "The role and relevance of mast cells in urticaria." Immunol Rev **282**(1): 232-247.

Craig, S. S. and L. B. Schwartz (1989). "Tryptase and chymase, markers of distinct types of human mast cells." Immunol Res **8**(2): 130-148.

Dallos, P., M. C. Billone, J. D. Durrant, C. Wang and S. Raynor (1972). "Cochlear inner and outer hair cells: functional differences." Science **177**(4046): 356-358.

Derebery, M. J. and K. I. Berliner (2000). "Prevalence of allergy in Meniere's disease." Otolaryngol Head Neck Surg **123**(1 Pt 1): 69-75.

Derebery, M. J. and K. I. Berliner (2010). "Allergy and its relation to Meniere's disease." Otolaryngol Clin North Am **43**(5): 1047-1058.

Driver, E. C. and M. W. Kelley (2020). "Development of the cochlea." Development **147**(12).

Dvorak, A. M., R. A. Monahan, J. E. Osage and G. R. Dickersin (1980). "Crohn's disease: transmission electron microscopic studies. II. Immunologic inflammatory response. Alterations of mast cells, basophils, eosinophils, and the microvasculature." Hum Pathol **11**(6): 606-619.

Eady, R. A., T. Cowen, T. F. Marshall, V. Plummer and M. W. Greaves (1979). "Mast cell population density, blood vessel density and histamine content in normal human skin." Br J Dermatol **100**(6): 623-633.

Ehrlich, P. (1877). "Beiträge zur Kenntniss der Anilinfärbungen und ihrer Verwendung in der mikroskopischen Technik." Archiv für mikroskopische Anatomie **13**(1): 263-277.

Ekdale, E. G. (2016). "Form and function of the mammalian inner ear." J Anat **228**(2): 324-337.

Enerbäck, L. (1966). "Mast cells in rat gastrointestinal mucosa. I. Effects of fixation." Acta Pathol Microbiol Scand **66**(3): 289-302.

Eshhar, Z., M. Ofarim and T. Waks (1980). "Generation of hybridomas secreting murine reaginic antibodies of anti-DNP specificity." J Immunol **124**(2): 775-780.

Fay, R. R. (2012). Comparative hearing: mammals, Springer Science & Business Media.

Ferry, X., S. Brehin, R. Kamel and Y. Landry (2002). "G protein-dependent activation of mast cell by peptides and basic secretagogues." Peptides **23**(8): 1507-1515.

Fettiplace, R. (2017). "Hair Cell Transduction, Tuning, and Synaptic Transmission in the Mammalian Cochlea." Compr Physiol **7**(4): 1197-1227.

Fettiplace, R. and C. M. Hackney (2006). "The sensory and motor roles of auditory hair cells." Nat Rev Neurosci **7**(1): 19-29.

Fettiplace, R. and K. X. Kim (2014). "The physiology of mechanoelectrical transduction channels in hearing." Physiol Rev **94**(3): 951-986.

Galli, S. J., N. Borregaard and T. A. Wynn (2011). "Phenotypic and functional plasticity of cells of innate immunity: macrophages, mast cells and neutrophils." Nature Immunology **12**(11): 1035-1044.

Galli, S. J., J. Kalesnikoff, M. A. Grimbaldeston, A. M. Piliponsky, C. M. Williams and M. Tsai (2005). "Mast cells as "tunable" effector and immunoregulatory cells: recent advances." Annu Rev Immunol **23**: 749-786.

Galli, S. J. and Y. Kitamura (1987). "Genetically mast-cell-deficient W/Wv and Sl/Sld mice. Their value for the analysis of the roles of mast cells in biologic responses in vivo." Am J Pathol **127**(1): 191-198.

Galli, S. J., M. Maurer and C. S. Lantz (1999). "Mast cells as sentinels of innate immunity." Curr Opin Immunol **11**(1): 53-59.

Galli, S. J. and M. Tsai (2012). "IgE and mast cells in allergic disease." Nat Med **18**(5): 693-704.

Goines, L. and L. Hagler (2007). "Noise pollution: a modem plague." South Med J **100**(3): 287-294.

Gonçalves, M. S., A. F. Silveira, A. R. Teixeira and M. A. Hyppolito (2013). "Mechanisms of cisplatin ototoxicity: theoretical review." J Laryngol Otol **127**(6): 536-541.

González-de-Olano, D. and I. Álvarez-Twose (2018). "Mast Cells as Key Players in Allergy and Inflammation." J Investig Allergol Clin Immunol **28**(6): 365-378.

Grimbaldeston, M. A., C. C. Chen, A. M. Piliponsky, M. Tsai, S. Y. Tam and S. J. Galli (2005). "Mast cell-deficient W-sash c-kit mutant Kit W-sh/W-sh mice as a model for investigating mast cell biology in vivo." Am J Pathol **167**(3): 835-848.

Havia, M., E. Kentala and I. Pyykkö (2002). "Hearing loss and tinnitus in Meniere's disease." Auris Nasus Larynx **29**(2): 115-119.

Heiger-Bernays, W. J., J. M. Essigmann and S. J. Lippard (1990). "Effect of the antitumor drug cis-diamminedichloroplatinum(II) and related platinum complexes on eukaryotic DNA replication." Biochemistry **29**(36): 8461-8466.

Irani, A. M., S. I. Butrus, K. F. Tabbara and L. B. Schwartz (1990). "Human conjunctival mast cells: distribution of MCT and MCTC in vernal conjunctivitis and giant papillary conjunctivitis." J Allergy Clin Immunol **86**(1): 34-40.

Jamur, M. C. and C. Oliver (2011). "Origin, maturation and recruitment of mast cell precursors." Front Biosci (Schol Ed) **3**(4): 1390-1406.

Jordan, P. and M. Carmo-Fonseca (2000). "Molecular mechanisms involved in cisplatin cytotoxicity." Cell Mol Life Sci **57**(8-9): 1229-1235.

Karayay, B., H. Olze and A. J. Szczepek (2023). "Degranulation of Murine Resident Cochlear Mast Cells: A Possible Factor Contributing to Cisplatin-Induced Ototoxicity and Neurotoxicity." Int J Mol Sci **24**(5).

Kashem, S. W., H. Subramanian, S. J. Collington, P. Magotti, J. D. Lambris and H. Ali (2011). "G protein coupled receptor specificity for C3a and compound 48/80-induced degranulation in human mast cells: roles of Mas-related genes MrgX1 and MrgX2." Eur J Pharmacol **668**(1-2): 299-304.

Kawakami, T. and S. J. Galli (2002). "Regulation of mast-cell and basophil function and survival by IgE." Nat Rev Immunol **2**(10): 773-786.

Kelland, L. (2007). "The resurgence of platinum-based cancer chemotherapy." Nat Rev Cancer **7**(8): 573-584.

Kinet, J. P. (1999). "The high-affinity IgE receptor (Fc epsilon RI): from physiology to pathology." Annu Rev Immunol **17**: 931-972.

Kitamura, Y., T. Kasugai, N. Arizono and H. Matsuda (1993). "Development of mast cells and basophils: processes and regulation mechanisms." Am J Med Sci **306**(3): 185-191.

Kitamura, Y., K. Oboki and A. Ito (2007). "Development of mast cells." Proc Jpn Acad Ser B Phys Biol Sci **83**(6): 164-174.

Kitamura, Y., T. Sonoda, T. Nakano, C. Hayashi and H. Asai (1985). "Differentiation processes of connective tissue mast cells in living mice." Int Arch Allergy Appl Immunol **77**(1-2): 144-150.

Lanvers-Kaminsky, C., A. A. Zehnhoff-Dinnesen, R. Parfitt and G. Ciarimboli (2017). "Drug-induced ototoxicity: Mechanisms, Pharmacogenetics, and protective strategies." Clin Pharmacol Ther **101**(4): 491-500.

Lim, R. and A. M. Brichta (2016). "Anatomical and physiological development of the human inner ear." Hear Res **338**: 9-21.

Lundequist, A. and G. Pejler (2011). "Biological implications of preformed mast cell mediators." Cell Mol Life Sci **68**(6): 965-975.

Mann, Z. F. and M. W. Kelley (2011). "Development of tonotopy in the auditory periphery." Hear Res **276**(1-2): 2-15.

Marone, G., M. Triggiani, A. Genovese and A. De Paulis (2005). "Role of human mast cells and basophils in bronchial asthma." Adv Immunol **88**: 97-160.

McNeil, B. D., P. Pundir, S. Meeker, L. Han, B. J. Undem, M. Kulka and X. Dong (2015). "Identification of a mast-cell-specific receptor crucial for pseudo-allergic drug reactions." Nature **519**(7542): 237-241.

Meech, R. P., K. C. Campbell, L. P. Hughes and L. P. Rybak (1998). "A semiquantitative analysis of the effects of cisplatin on the rat stria vascularis." Hear Res **124**(1-2): 44-59.

Mekada, K., K. Abe, A. Murakami, S. Nakamura, H. Nakata, K. Moriwaki, Y. Obata and A. Yoshiki (2009). "Genetic differences among C57BL/6 substrains." Exp Anim **58**(2): 141-149.

Metcalfe, D. D., D. Baram and Y. A. Mekori (1997). "Mast cells." Physiol Rev **77**(4): 1033-1079.

Metz, M. and M. Maurer (2007). "Mast cells--key effector cells in immune responses." Trends Immunol **28**(5): 234-241.

Mulero, I., M. P. Sepulcre, J. Meseguer, A. García-Ayala and V. Mulero (2007). "Histamine is stored in mast cells of most evolutionarily advanced fish and regulates the fish inflammatory response." Proc Natl Acad Sci U S A **104**(49): 19434-19439.

Nadler, M. J., S. A. Matthews, H. Turner and J. P. Kinet (2000). "Signal transduction by the high-affinity immunoglobulin E receptor Fc epsilon RI: coupling form to function." Adv Immunol **76**: 325-355.

Ogasawara, H., M. Furuno, K. Edamura and M. Noguchi (2019). "Novel MRGPRX2 antagonists inhibit IgE-independent activation of human umbilical cord blood-derived mast cells." J Leukoc Biol **106**(5): 1069-1077.

Palomäki, V. A. and J. T. Laitinen (2006). "The basic secretagogue compound 48/80 activates G proteins indirectly via stimulation of phospholipase D-lysophosphatidic acid receptor axis and 5-HT1A receptors in rat brain sections." Br J Pharmacol **147**(6): 596-606.

Payan, P., H. Kossmann, A. Watrin, N. Mayer-Gostan and G. Boeuf (1997). "Ionic composition of endolymph in teleosts: origin and importance of endolymph alkalinity." J Exp Biol **200**(Pt 13): 1905-1912.

Rabinowitz, P. M. (2000). "Noise-induced hearing loss." Am Fam Physician **61**(9): 2749-2756, 2759-2760.

Roberts-Thomson, I. C., J. Fon, W. Uylaki, A. G. Cummins and S. Barry (2011). "Cells, cytokines and inflammatory bowel disease: a clinical perspective." Expert Rev Gastroenterol Hepatol **5**(6): 703-716.

Rybak, L. P. (2007). "Mechanisms of cisplatin ototoxicity and progress in otoprotection." Curr Opin Otolaryngol Head Neck Surg **15**(5): 364-369.

Schulman, E. S., D. W. MacGlashan, Jr., S. P. Peters, R. P. Schleimer, H. H. Newball and L. M. Lichtenstein (1982). "Human lung mast cells: purification and characterization." J Immunol **129**(6): 2662-2667.

Shi, L., Y. Chang, X. Li, S. Aiken, L. Liu and J. Wang (2016). "Cochlear Synaptopathy and Noise-Induced Hidden Hearing Loss." Neural Plast **2016**: 6143164.

So, H., H. Kim, J. H. Lee, C. Park, Y. Kim, E. Kim, J. K. Kim, K. J. Yun, K. M. Lee, H. Y. Lee, S. K. Moon, D. J. Lim and R. Park (2007). "Cisplatin cytotoxicity of auditory cells requires secretions of proinflammatory cytokines via activation of ERK and NF-kappaB." J Assoc Res Otolaryngol **8**(3): 338-355.

Sperr, W. R., H. C. Bankl, G. Mundigler, G. Klappacher, K. Grossschmidt, H. Agis, P. Simon, P. Laufer, M. Imhof, T. Radaszkiewicz, D. Glogar, K. Lechner and P. Valent (1994). "The human cardiac mast cell: localization, isolation, phenotype, and functional characterization." Blood **84**(11): 3876-3884.

St. John, A. L., A. P. S. Rathore and F. Ginhoux (2023). "New perspectives on the origins and heterogeneity of mast cells." Nature Reviews Immunology **23**(1): 55-68.

Sterkers, O., E. Ferrary and C. Amiel (1988). "Production of inner ear fluids." Physiol Rev **68**(4): 1083-1128.

Strattan, E., S. Palaniyandi, R. Kumari, J. Du, N. Hakim, T. Huang, M. V. Kesler, C. D. Jennings, J. L. Sturgill and G. C. Hildebrandt (2019). "Mast Cells Are Mediators of Fibrosis and Effector Cell Recruitment in Dermal Chronic Graft-vs.-Host Disease." Front Immunol **10**: 2470.

Strobel, S., H. R. Miller and A. Ferguson (1981). "Human intestinal mucosal mast cells: evaluation of fixation and staining techniques." J Clin Pathol **34**(8): 851-858.

Szczepek, A. J., T. Dudnik, B. Karayay, V. Sergeeva, H. Olze and A. Smorodchenko (2020). "Mast Cells in the Auditory Periphery of Rodents." Brain Sci **10**(10).

Tatemoto, K., Y. Nozaki, R. Tsuda, S. Konno, K. Tomura, M. Furuno, H. Ogasawara, K. Edamura, H. Takagi, H. Iwamura, M. Noguchi and T. Naito (2006). "Immunoglobulin E-independent activation of mast cell is mediated by Mrg receptors." Biochem Biophys Res Commun **349**(4): 1322-1328.

Varricchi, G., Francesca W. Rossi, Maria R. Galdiero, F. Granata, G. Criscuolo, G. Spadaro, A. de Paulis and G. Marone (2019). "Physiological Roles of Mast Cells: Collegium Internationale Allergologicum Update 2019." International Archives of Allergy and Immunology **179**(4): 247-261.

Virk, H., G. Arthur and P. Bradding (2016). "Mast cells and their activation in lung disease." Transl Res **174**: 60-76.

Wang, D. and S. J. Lippard (2005). "Cellular processing of platinum anticancer drugs." Nat Rev Drug Discov **4**(4): 307-320.

Wolters, P. J., J. Mallen-St Clair, C. C. Lewis, S. A. Villalta, P. Baluk, D. J. Erle and G. H. Caughey (2005). "Tissue-selective mast cell reconstitution and differential lung gene expression in mast cell-deficient Kit(W-sh)/Kit(W-sh) sash mice." Clin Exp Allergy **35**(1): 82-88.

Wulf, E., A. Deboben, F. A. Bautz, H. Faulstich and T. Wieland (1979). "Fluorescent phallotoxin, a tool for the visualization of cellular actin." Proc Natl Acad Sci U S A **76**(9): 4498-4502.

Yoshioka, T. and M. Sakakibara (2013). "Physical aspects of sensory transduction on seeing, hearing and smelling." Biophysics (Nagoya-shi) **9**: 183-191.

Yu, X., R. Man, Y. Li, Q. Yang, H. Li, H. Yang, X. Bai, H. Yin, J. Li and H. Wang (2019). "Paeoniflorin protects spiral ganglion neurons from cisplatin-induced ototoxicity: Possible relation to PINK1/BAD pathway." J Cell Mol Med **23**(8): 5098-5107.

Zeng, B., E. Domarecka, L. Kong, H. Olze, J. Scheffel, S. Moñino-Romero, F. Siebenhaar and A. J. Szczepek (2024). "A systematic review of the clinical evidence for an association between type I hypersensitivity and inner ear disorders." Front Neurol **15**: 1378276.

Statutory Declaration

“I, Bin Zeng, by personally signing this document in lieu of an oath, hereby affirm that I prepared the submitted dissertation on the topic “Function and regulation of mast cells in the inner ear and applications to mast cell-driven diseases (in English). Funktion und Regulation von Mastzellen im Innenohr und Anwendungen bei Mastzellen-bedingten Krankheiten (in German)”, independently and without the support of third parties, and that I used no other sources and aids than those stated.
All parts which are based on the publications or presentations of other authors, either in letter or in spirit, are specified as such in accordance with the citing guidelines. The sections on methodology (in particular regarding practical work, laboratory regulations, statistical processing) and results (in particular regarding figures, charts and tables) are exclusively my responsibility.

Furthermore, I declare that I have correctly marked all of the data, the analyses, and the conclusions generated from data obtained in collaboration with other persons, and that I have correctly marked my own contribution and the contributions of other persons (cf. declaration of contribution). I have correctly marked all texts or parts of texts that were generated in collaboration with other persons.

My contributions to any publications to this dissertation correspond to those stated in the below joint declaration made together with the supervisor. All publications created within the scope of the dissertation comply with the guidelines of the ICMJE (International Committee of Medical Journal Editors; http://www.icmje.org) on authorship. In addition, I declare that I shall comply with the regulations of Charité – Universitätsmedizin Berlin on ensuring good scientific practice.

I declare that I have not yet submitted this dissertation in identical or similar form to another Faculty.

The significance of this statutory declaration and the consequences of a false statutory declaration under criminal law (Sections 156, 161 of the German Criminal Code) are known to me.”

Date Signature

Curriculum Vitae

My curriculum vitae does not appear in the electronic version of my paper for reasons of data protection

Acknowledgments

First, I would like to thank Prof. Dr. Marcus Maurer for providing me with the valuable opportunity to pursue my doctoral degree at his institute.

I am sincerely grateful to Prof. Dr. Frank Siebenhaar, Prof. Dr. Agnieszka Szczepek, Dr. Sherezade Moñino-Romero, and Dr. Jörg Scheffel for their continuous guidance, help, and encouragement with my doctoral studies. They are the shining lighthouse on my scientific path. Their profound knowledge has given me unwavering strength and tirelessly guided me forward.

In addition, I would like to thank Dr. Stefan Frischbutter, Niklas Amadeus Mahnke, and Friederike Petzhold in our laboratory, as well as Ewa Domarecka, Julia Fuchs, Olga Hegend, Lingyi Kong and Rebeca Kristein from the group of Prof. Dr. Agnieszka Szczepek for their kind assistance during the project. I am honored to have worked with such two wonderful teams.

I would also like to thank my dear friends and lovely family for their company and unwavering support!